Journal of Optimization in Industrial Engineering
Vol.16, Issue 1, Winter & Spring 2023, 167–184
DOI10.22094/JOIE.2023.1974939.2022

Research Article

Optimizing Investment of Pumped Hydro Storage System for Renewable Energy Future

Zohreh Goudarzi[a], Jafar Bagherinejad[b,*], Majid Rafiee[c], Amir Abolfazl Suratgar[d]

[a] *Ph. D. student of Industrial Engineering, Department of Industrial Engineering, Faculty of Engineering, Alzahra University, Tehran, Iran.*
[b,*] *Associate Professor of Industrial Engineering, Department of Industrial Engineering, Faculty of Engineering, Alzahra University, Tehran, Iran.*
[c] *Associate Professor of Industrial Engineering, Department of Industrial Engineering, Sharif University of Technology, Tehran, Iran.*
[d] *Associate Professor of Electrical Engineering, Department of Electrical Engineering, Amirkabir University of Technology, Tehran, Iran.*

Received 13 December 2022; Revised 10 March 2023; Accepted 14 March 2023

Abstract

Renewable energies are increasingly being considered for use in electricity networks. The high variability of consumption, and the instability of renewable energies, necessitate the use of energy storage systems. The problem of optimizing investment for an energy storage system is formulated here. The proposed model, in particular, determines the optimal size of the energy storage system based on maximizing social welfare. The problem is formulated as a mixed-integer linear programming (MILP), and an equivalent mixed complementary problem (MCP) to solve a quadratic system of nonlinear equations. Due to its high efficiency, the Benders decomposition technique is used to solve the proposed model. The results of solving a 300-node system that cannot be solved by CPLEX using the Benders decomposition technique are presented. The results demonstrate that the proposed method can efficiently find a solution while considering the network's limitations, increasing social welfare. Finally, the performance of the MILP and MCP models for various numerical cases is compared. The findings of this paper indicate that by increasing the dimensions of the problem, the performance of the MCP model improves compared to the MILP model in terms of computational time and the value of the objective function.

Keywords: Energy storage system; Optimal sizing; Mixed complementary problem; Benders decomposition.

1. Introduction

Because of rising electrical energy consumption and growing concerns about climate change, Renewable Energy (RE) resources have received extensive attention in recent decades (Benalcazar, 2021). However, because RE sources are unpredictable and random, they cannot be used solely to meet the electricity demand, particularly during peak consumption periods. Therefore, large-scale electrical energy generated by thermal, hydroelectric, and nuclear power plants remains a primary source near the nominal load. Only by utilizing large storage capacities and long transmission lines can RE sources compensate for the network's spatial and temporal variability of power demand. That is why Energy Storage System (ESS) has been proposed as a solution to this problem (Gardiner et al., 2020).

Some examples are Pumped-Hydro Storage (PHS), batteries, compressed-air energy storage, flywheel energy storage, and other ESSs. PHS has the world's highest production and storage capacity (Hunt et al., 2022), making it well-suited for large-scale RE systems. The PHS also has a high energy storage capacity, low start-up costs in both pumping and production modes, and a long lifespan (50-100 years) (Guittet et al., 2016). In 2018, hundreds of PHS power plants with a total capacity of approximately 160.3 GW were installed worldwide (Hunt et al., 2022). PHS systems are available in both closed-loop and open-loop configurations. The upper and lower reservoirs in closed-loop systems are at different heights, whereas the lower reservoir in open-loop systems can be a river, sea, or other body of water.

1.1. Motivation

Based on location and capacity, storage systems can provide services and benefits such as flexibility, arbitrage, and network expansion delay. The PHS system can be considered a power plant that stores excess electricity generated by base power plants and converts it to peak power. Furthermore it reduces energy consumption and production costs in base-loaded power plants (thermal and nuclear) and the need to install peak power plants (generally gas-fired). As summarized in several review articles and special editorial issues, the topic has recently attracted several studies (Arteaga et al., 2021; Nazari et al., 2021; Liu et al., 2021). The most pressing problems in the study of ESSs are those concerning sizing, siting, storage operation, and investment in electricity networks (Fertig et al., 2014; Rehman et al., 2015; Hassan & Dvorkin 2018; Saber et al., 2018; Mousavi et al., 2019).

Inetwork constraints influence location decisions in the case of PHS allocation. Storage operations and investment decisions depend on the storage facility's size (capacity) and location. With that being said, the most critical issue

*Corresponding author Email address: jbagheri@alzahra.ac.ir

is determining the required investment for private sector participation in this field. In this regard, the energy storage system's size must be determined to achieve maximum efficiency with the minimum necessary investment (Arteaga et al., 2021). It is essential to consider the constraints the network's constraints as much as possible to achieve this goal.

1.2. Related work

This section reviews the most recent and relevant studies from the vast literature. Gravelle (1976) and Nguyan (1976) thought about peak and non-peak period models. They assumed that the sold electricity could be transferred between adjacent periods indefinitely for fixed unit costs. Gravelle (1976) established the fundamental analytical structure, including necessary and sufficient conditions for optimal storage, pricing, and capacity. The results of Nguyan (1976) indicate that fewer electricity stations are used generally when storage facilities are used. The electricity price during peak hours is lower than without storage, resulting in significant welfare benefits.

A group of researchers investigated the investment of ESS in power systems. Based on their goal, they can be divided into two categories. In the first category, ESS investment decisions in wholesale electricity markets are made to maximize the merchant's profit (Fertig et al., 2014; Dvorkin et al., 2018; Huang et al., 2020; Abadie & Goicoechea, 2022). Fertig et al. (2014) explored PHS system investment capacity and scheduling optimization. They used real options theory to evaluate investment opportunities to maximize profit. A tri-level model in the market-based electricity system was presented by Dvorkin et al (2018). They jointly optimized the size and site of electromechanical storage. At the upper level, the objective was to maximize the lifetime profit from storage while assuming a constant rate of return on investment. At the mid-level, the cost of transmission development decisions and the expected operating cost of the system is minimized. Finally, the maximization of social welfare is considered at a lower level, while the impact of power fluctuations on the real-time profitability of the storage was not considered. In Huang et al. (2020), Stackelberg competition in wholesale electricity markets was proposed as a tri-level optimization problem. The upper level is concerned with profit maximization, while the middle level decides on the regulated ESS investment. At the lower level, the social planner decides on the economic dispatch and overall storage operations to minimize the total cost. The effect of an optimal management strategy on prices under the uncertainty conditions for the PHS system was studied using a mean-reverting jump-diffusion stochastic model of electricity prices (Abadie & Goicoechea, 2022).

The second category, which focuses on optimal social investment, seeks to minimize the total system costs (ESS investment and generation costs). These costs are minimized by making ESS investment decisions that determine the optimal location and size for the system. Social planners, like the government, frequently make these investment decisions (Steffen & Weber, 2013; Korpås & Botterud, 2020; Spisto & Hrelja, 2016; Xu et al., 2017; Zhang & Conejo, 2018; Javed et al., 2020; Canales et al., 2021; Liu et al., 2021; Haas et al., 2022). It was assumed by Steffen & Weber (2013) and Korpås & Botterud (2020) that electricity could be purchased whenever the price is low and sold when the price rises. They proposed a capacity portfolio planning model for the power network to determine the most efficient storage capacity by minimizing total costs. The proposed model by Steffen & Weber (2013) was applied to a case study in Germany. The dependence of capacity on cost parameters and the effect of CO_2 price on storage efficiency were investigated. The uncertainty of the demand was not considered in these studies. In this study, the economic feasibility of new investments in storage technologies, the environmental effects of CO_2 emissions, and the RE level were investigated by Spisto & Hrelja (2016). A case study of two regions of the Italian electricity market was conducted. The findings revealed that, despite lower costs, using PHS systems does not guarantee optimality regarding environmental effects. It would be preferable if the social value of the investment provided private profit.

Xu et al. (2017) developed a two-level model to optimize ESS size and site. This study minimized the system's total and operational costs at upper and lower levels. A robust optimization tool was developed to minimize the investment in storage units to invest in storage systems under uncertainty (Zhang & Conejo, 2018). The column-and-constraint generation algorithm was applied to solve robust optimization problems in a two-level model. In contrast, the lower and upper levels were solved using complex integer linear programming and linear programming, respectively. The findings indicate that development decisions depend heavily on budget uncertainty and storage unit investment costs. The level of RE in the system, the economic feasibility of new investment in ESS, and their environmental impact were investigated by Javed et al. (2020). The paper proposed a hybrid Pumped Hydro and Battery Storage (PHBS) system to create a more reliable and stable PHBS system.

Canales et al. (2021) present a multi-objective optimization model for determining the optimal size and evaluating the performance of the hybrid battery-pumped storage. The proposed model simultaneously considers reducing energy costs and increasing reliability. The results of a case study on Ometepe island, Nicaragua, demonstrated that the energy cost and optimal power system size are affected by different levels of the capital cost associated with hybrid battery-pumped storage. Liu et al. (2021) used a Non-dominated Sorting Genetic Algorithm with Elite Strategy (NSGA-II) to optimize a wind power system integrated with the PHS system. Their objective was to calculate the size of a PHS integrated with a high-capacity wind farm. The results showed that the income from selling electricity does not always equal the increase in investment. The economic potential of the

PHS system was evaluated in stages to minimize costs (Haas et al., 2022). The authors began by reviewing various sites using a Geographic Information System (GIS)-based method. The cost-potential curves are then plotted using the estimated costs for each site. Finally, the curves evaluate each site's impact on investment recommendations. Based on their findings, most PHS sites were significantly less expensive than current lithium-ion battery systems, even when battery prices were rapidly declining.

Several papers were also dedicated to integrating photovoltaic and PHS systems (Lin et al., 2020; Yang et al., 2021). According to the findings of Lin et al. (2020), the initial investment required to meet the demand for residents of villas and apartments using a PV-PHS system is 35,417 and 36,423 Chinese yuan, with a payback period of 9.01 and 7.06 years, respectively. Yang et al. (2021) demonstrated that the payback period for a PV-PHS system in rural homes in China is approximately 6.4-8.1 years, and the annual net income per family is 314.2-541.6 Chinese yuan.

Several papers in this field have also studied PHS issues analytically. Gaudard (2015) presented an economic and financial analysis of the deployment of a PHS system based on a Swiss case study. This analysis shows that under current market conditions, such an investment is not profitable, and most of the time, higher price fluctuations cause a reduction in annual income. Barbour et al. (2016) examined the evolution of PHS in several notable electricity markets and compared several mechanisms that can reward PHS in various international market frameworks. Liu and Woo (2017) studied the profitability of PHS systems and renewable generation in California. They demonstrated that increased RE generation does not reduce the PHS system's operating profit. However, the investment incentive was low because its annual operating profit was nearly equal to its fixed costs.

The drivers and barriers to PHS use are classified as technological-environmental and socio-economic (Ali et al., 2021). According to this classification, network flexibility (i.e., energy time-shifting), income generation, and rural development (i.e., job opportunities) are the most critical drivers. Barriers include a lack of good infrastructure (i.e., transmission lines) and difficulties obtaining the initial and ongoing capital required for investment. According to this study, the most significant barrier is high investment costs with a global weight of 0.0963 compared to all other barriers.

There is still a lack of studies considering the issue of PHS investment with network constraints, and a practical and appropriate model is still missing. Integrating PHS into electricity networks to provide needed electricity during peak hours ultimately increases social welfare. Therefore, the current study investigates the necessary investment in PHS to maximize social welfare.

Nomenclature

A. Indices

R	RE generators ($R = 1,2, \dots, r$)
F	Conventional generators ($F = 1,2, \dots, f$)
S	PHS systems ($S = 1,2, \dots, s$)
L	Transmission lines ($L = 1,2, \dots, l$)
D	Demand units ($D = 1,2, \dots, d$)
N	Buses ($N = 1,2, \dots, n$)
Y	Lifetime ($Y = 1,2, \dots, y$)
H	Time period ($H = 1,2, \dots, h$)
i	Interest rate (%)
j	The bus number that the unit connects to the network
n^{org}	n is the originating bus for line l
n^{ter}	n is the terminating bus for line l
B. Parameters	
$P^{(MAX)}$	Maximum market price [$ per MWh]
T	Number of block hours presenting one year
M	A big constant number
VC_f	The marginal operation cost of a conventional generator [$ per MWh]
$RC_f^{(UP)}$	Positive marginal reserve cost of a conventional generator [$ per MWh]
$RC_f^{(DN)}$	Negative marginal reserve cost of a conventional generator [$ per MWh]
$K_f^{(MAX)}$	The maximum capacity of a conventional generator [MW]
IG_f	The initial generation of a conventional generator [MWh]
RA_f	Ramping capacity of a conventional generator [MWh]
V_r	The marginal operation cost of a RE generator [$ per MWh]
IG_r	The initial generation of a RE generator [MWh]
RA_r	Ramping capacity of a RE generator [MWh]
$Q_{r,y,h}$	Hourly accessibility of a RE generator [%]
$K_{r,y,h}^{(MAX)}$	The maximum capacity of a RE generator [MW]
$FC_s^{(CAP)}$	Investment cost of the PHS generator/pump capacity [$ per MWh]
$FC_s^{(EN)}$	Investment cost of the PHS reservoir size [$ per MWh]
$RC_s^{(UP)}$	Positive marginal reserve cost of the PHS [$ per MWh]
$RC_s^{(DN)}$	Negative marginal reserve cost of the PHS [$ per MWh]
$E^{(ST)}$	The initial stored energy [MW]
SL_s	The PHS conversion efficiency [%]
$CH_s^{(MIN)}$	The minimum charge level of the PHS [MW]
$DCH_s^{(MIN)}$	The minimum discharge level of the PHS [MW]
$K_s^{(MAX)}$	The maximum generator/pump capacity of the PHS [MW]

$E_s^{(MAX)}$	The maximum reservoir size of the PHS [MW]
$K_l^{(MAX)}$	The maximum flow limit for the transmission line [MW]
$D_{d.v.h}^{(MAX)}$	Demand data [MWh]
PS_y	Positive spinning reserve required [MW]
NS_y	Negative spinning reserve required [MW]
$H_{l,n}$	The Power Transfer Distribution Factor (PTDF) matrix
$A_{n,s}$	PHS-bus incidence matrix
$B_{n,s}$	PHS-bus incidence matrix
$C_{n,f}$	Generator-bus incidence matrix
$D_{n,d}$	Demand-bus incidence matrix
C. Variables	
$gen_{f,y,h}$	Power production by the conventional generator [MW]
$\alpha_{f,y,h}$	Lagrange multiplier associated with the conventional generator capacity
$\phi_{f,y,h}^{(1)}$	Ramp-up constraint factor for the conventional generator output
$\phi_{f,y,h}^{(2)}$	Ramp-down constraint factor for the conventional generator output
$gen_{r,y,h}$	Power production by the RE generator [MW]
$\beta_{r,y,h}$	Lagrange multiplier associated with the RE generator capacity (energy-based)
$\phi_{r,y,h}^{(1)}$	Ramp-up constraint factor for the RE generator
$\phi_{r,y,h}^{(2)}$	Ramp-down constraint factor for the RE generator
$ch_{s,v,h}$	The charge level of the PHS [MW]
$dch_{s,v,h}$	The discharge level of the PHS [MW]
$e_{s,y,h}^{(st)}$	Stored energy at the end of the time step of the PHS [MW]
$e_{s,v}^{(in)}$	The PHS reservoir size [MWh]
$k_{s,v}^{(in)}$	The PHS capacity [MWh]
$\mu_{s,y,h}$	Lagrange multiplier associated with the PHS size
$\iota_{s,y,h}$	Lagrange multiplier associated with the PHS capacity
$\delta_{s,y,h}$	Lagrange multiplier associated with the minimum charge level
$\varpi_{s,y,h}$	Lagrange multiplier associated with the minimum discharge level
$\psi_{s,y}$	Lagrange multiplier associated with the maximum allowed investment in the PHS capacity
$\nu_{s,y}$	Lagrange multiplier associated with the maximum allowed investment in the PHS size
$\vartheta_{s,y}$	Lagrange multiplier associated with the capacity difference between two consecutive years
$\varsigma_{s,y,h}$	The auxiliary variable representing the product of $\omega_{s,v,h}^1 \times k_s^{(in)}$
$\kappa_{s,y,h}$	The auxiliary variable representing the product of $\omega_{s,v,h}^2 \times k_s^{(in)}$
$flow_{l,y,h}$	Power flow through the transmission line [MW]
$\varrho_{l,y,h}$	Lagrange multiplier associated with the capacity limit of the line
$\pi_{l,y,h}$	Lagrange multiplier associated with the capacity limit of the line
$ld_{d,v,h}$	Load [MW]
$\tau_{d,y,h}$	Lagrange multiplier associated with the load capacity
$\eta_{y,h}$	Lagrange multiplier associated with the spinning reserve (upward regulation)
$\zeta_{y,h}$	Lagrange multiplier associated with the spinning reserve (down upward regulation)
D. Binary Variables	
$\omega_{s,y,h}^1$	The binary variable indicates that the PHS is discharging
$\omega_{s,y,h}^2$	The binary variable indicates that the PHS is charging
E. Free sign Variables	
$\xi_{s,y,h}$	Value of stored energy (Lagrange multiplier associated with the water-balance constraint)
$\lambda_{y,h}$	Electricity price (Lagrange multiplier associated with the electrical-energy balance constraint)
$\chi_{l,y,h}$	Lagrange multiplier associated with the line flow constraint
SW	Social welfare [$]
PR	Profit [$]

1.3. Contribution

This paper contributes to the relevant literature as follows. First, it proposes a mixed-integer linear programming (MILP) model for centralized Vertically Integrated Utility-based (VIU-based) investment in the PHS system. The original MILP model is then converted to an LP model, reducing its computational complexity. The outcomes of this LP model can be used as the benchmark for maximizing social welfare in relevant studies.

Second, it proposes a mixed complementary problem (MCP) model for decentralized market-based PHS investment. Profit-maximizing PHS system owners can use the MCP model results for market-based investment studies.

Third, the standard Benders decomposition algorithm is adopted to efficiently solve the LP and MCP models proposed in this paper.

The remainder of this paper is organized as follows. Section 2 establishes the LP model of PHS investment. Section 3 presents the equivalent MCP model. Section 4 discussed the Benders decomposition method’s applied solution techniques. Section 5 examines an illustrative example and IEEE case studies. Finally, the paper is concluded in Section 6.

2. LP model of PHS Investment

The MILP model is used for system optimization because it is a powerful and flexible method for solving large and complex problems. MILP model is a common language for uniquely describing a problem in exact mathematical terms. This model necessitates simplification and the development of methods for constraining the solution space and determining the global solution.

The optimal PHS capacity must be coordinated with the current and future capacity of generators, loads, and the transmission network to maximize social welfare in the electricity industry.

First, a MILP model for calculating the optimal capacity of the PHS is proposed in this section. The equivalent LP model is then presented. The optimal PHS capacity modeling is based on the endogenous modeling of loads and transmission network capacities. More specifically, the capacity development of conventional and renewable-energy generators is endogenously modeled[1]. The main components of the PHS investment model will be explained in the following sections.

2.1. Objective function

This MILP model can be used to calculate the optimal PHS capacity and reservoir size that maximizes the social welfare of the electricity market:

$$Maximize\ SW = \sum_y(\sum_h \sum_d(P^{(MAX)}\, ld_{d,y,h}T) - \sum_h \sum_f(VC_f\, gen_{f,y,h}T) - \sum_h \sum_f(RC_f^{(UP)}T[K_f^{(MAX)} - gen_{f,y,h}]) - \sum_h \sum_f(RC_f^{(DN)}T[K_f^{(MAX)} - gen_{f,y,h}]) - \sum_h \sum_r(V_r gen_{r,y,h}T) - \sum_s(FC_s^{(CAP)} k_{s,y=Y}^{(in)}) - \sum_s(FC_s^{(EN)} e_{s,y}^{(in)}) - \sum_h \sum_s(RC_s^{(UP)}[k_{s,y}^{(in)} - dch_{s,y,h}]) - \sum_h \sum_s(RC_s^{(DN)}[k_{s,y}^{(in)} - ch_{s,y,h}]))/(1+i)^{y-1} \quad (1)$$

The proposed optimization model's objective function, which includes utility and unit costs, is depicted in (1). The first term refers to the utility of satisfying the demand. In contrast, others refer to costs associated with conventional, renewable, and PHS, which aim to maximize the difference between utility and costs to maximize social welfare. The following sections discuss the constraints that must be considered.

2.2. The conventional generators

There are two types of generator constraints: generation capacity (2) and ramp-rate constraints (3-6). The maximum capacity limits the amount of output per generator unit per hour.

$$gen_{f,y,h} \le K_f^{(MAX)} \qquad \forall f,y,h \qquad (2)$$

For each conventional generator, the up and down ramping amount between two consecutive periods should be less than or equal to the corresponding ramp rate. These constraints are written with a default value for the first period.

$$gen_{f,y,h} - IG_f \le RA_f \qquad \forall f,y,h = 1 \qquad (3)$$

$$gen_{f,y,h} - gen_{f,y,h-1} \le RA_f \qquad \forall f,y,h > 1 \qquad (4)$$

$$IG_f - gen_{f,y,h} \le RA_f \qquad \forall f,y,h = 1 \qquad (5)$$

$$gen_{f,y,h-1} - gen_{f,y,h} \le RA_f \qquad \forall f,y,h = 1 \qquad (6)$$

2.3. The renewable-energy generators

We have the same two constraints (7-11) as conventional generators. The generation of renewable-energy generators is limited to the available RE.

$$gen_{r,y,h} \le Q_{r,y,h}K_{r,y,h}^{(MAX)} \qquad \forall r,y,h \qquad (7)$$

The following constraints represent each renewable technology's up and down ramping limits with corresponding flexibility rates. These constraints are also written for the first period with a default value for the amount of renewable technology production.

$$gen_{r,y,h} - IG_r \le RA_r \qquad \forall r,y,h = 1 \qquad (8)$$

$$gen_{r,y,h} - gen_{r,y,h-1} \le RA_r \qquad \forall r,y,h > 1 \qquad (9)$$

$$IG_r - gen_{r,y,h} \le RA_r \qquad \forall r,y,h = 1 \qquad (10)$$

$$gen_{r,y,h-1} - gen_{r,y,h} \le RA_r \qquad \forall r,y,h = 1 \qquad (11)$$

2.4. The PHS constraints

PHS systems are characterized by charge/discharge capacity (in MW), reservoir size (in MWh), and charge/discharge losses. The PHS systems' constraints include four components: water balance, charge, and discharge operation, charge and discharge capacity, and spinning reserve, which are as follows:

$$E^{(ST)} + SL_s ch_{s,y,h} - \frac{1}{SL_s} dch_{s,y,h} = e_{s,y,h}^{(st)} \qquad \forall s,y,h = 1 \qquad (12)$$

$$e_{s,y,h-1}^{(st)} + SL_s ch_{s,y,h} - \frac{1}{SL_s} dch_{s,y,h} = e_{s,y,h}^{(st)} \qquad \forall s,y,h > 1 \qquad (13)$$

$$e_{s,y,h}^{(st)} \le e_{s,y}^{(in)} \qquad \forall s,y,h \qquad (14)$$

Constraints (12-14) indicate the water-balance constraints of PHS that model the input and output water flow to and from a reservoir. For the first period, a default value is the amount of stored water in the reservoir. Also, the amount

[1] The capacity of loads and transmission network is modeled as parameters, while the capacity of conventional generators and RE generators are variables of the proposed MILP model.

of stored water should be less than or equal to the reservoir size (14).

$$\omega_{s,y,h}^{1} + \omega_{s,y,h}^{2} \leq 1 \qquad \forall s,y,h \qquad (15)$$

$$\omega_{s,y,h}^{1} + \omega_{s,y,h+1}^{2} \leq 1 \qquad \forall s,y,h \qquad (16)$$

$$\omega_{s,y,h+1}^{1} + \omega_{s,y,h}^{2} \leq 1 \qquad \forall s,y,h \qquad (17)$$

Eq (15) considers the PHS's non-simultaneous charge and discharge operation each hour. Constraints (16-17) show the minimum offline time required in PHS to switch from charge to discharge mode (or vice versa).

$$\omega_{s,y,h}^{1} DCH_{s}^{(MIN)} \leq dch_{s,y,h} \leq \omega_{s,y,h}^{1} k_{s,y}^{(in)} \qquad \forall s,y,h \qquad (18)$$

$$\omega_{s,y,h}^{2} CH_{s}^{(MIN)} \leq ch_{s,y,h} \leq \omega_{s,y,h}^{2} k_{s,y}^{(in)} \qquad \forall s,y,h \qquad (19)$$

Each generator and pump mode has its physical MW capacity (18-19).

$$k_{s,y}^{(in)} \leq K_{s}^{(MAX)} \qquad \forall s,y \qquad (20)$$

$$k_{s,y-1}^{(in)} \leq k_{s,y}^{(in)} \qquad \forall s,y \qquad (21)$$

$$e_{s,y}^{(in)} \leq E_{s}^{(MAX)} \qquad \forall s,y \qquad (22)$$

The optimal PHS generator/pump capacity and reservoir size are bounded by upper limits $K_{s}^{(MAX)}$ and $E_{s}^{(MAX)}$ (20-21). Also, constraint (21) ensures that the capacity per year ($k_{s,y}^{(in)}$) is equal to the previous year's capacity ($k_{s,y-1}^{(in)}$).

$$\sum_{s}(\omega_{s,y,h}^{1} k_{s,y}^{(in)} - dch_{s,y,h}) + \sum_{s}(ch_{s,y,h} - CH_{s}^{(MIN)}) + \sum_{f}(K_{f}^{(MAX)} - gen_{f,y,h}) + \sum_{d} ld_{d,y,h} \geq PS_{y} \qquad \forall y,h \qquad (23)$$

$$\sum_{s}(\omega_{s,y,h}^{2} k_{s,y}^{(in)} - ch_{s,y,h}) + \sum_{s}(dch_{s,y,h} - DCH_{s}^{(MIN)}) + \sum_{d}(D_{d,y,h}^{(MAX)} - ld_{d,y,h}) + \sum_{f} gen_{f,y,h} \geq NS_{y} \qquad \forall y,h \qquad (24)$$

Constraints (23-24) represent the PHS's reserve capacity for frequency-control service.

2.5. The load constraint

The consumption level must always be less than or equal to the maximum load (25).

$$ld_{d,y,h} \leq D_{d,y,h}^{(MAX)} \qquad \forall d,y,h \qquad (25)$$

2.6. The transmission network constraints

Constraint (26) ensures that the power flowing through a transmission line stays within the line's capacity limit. In addition, the power flowing through a line is calculated in (27) per hour (the flows are computed using the Power Transfer Distribution Factors (PTDF) matrix (Hesamzadeh et al., 2020)).

$$-K_{l}^{(MAX)} \leq flow_{l,y,h} \leq K_{l}^{(MAX)} \qquad \forall l,y,h \qquad (26)$$

$$\sum_{n}\sum_{s} H_{l,n} A_{n,s} dch_{s,y,h} - \sum_{n}\sum_{s} H_{l,n} B_{n,s} ch_{s,y,h} + \sum_{n}\sum_{f} H_{l,n} C_{n,f} gen_{f,y,h} - \sum_{n}\sum_{d} H_{l,n} D_{n,d} ld_{d,y,h} = flow_{l,y,h} \qquad \forall l,y,h \qquad (27)$$

2.7. The electrical-energy balance constraint

The constraint (28) ensures that the electricity generated per hour (from conventional, renewable, and PHSS sources) equals the load and PHS consumption (charge).

$$\sum_{f} gen_{f,y,h} + \sum_{s}(dch_{s,y,h} - ch_{s,y,h}) + \sum_{r} gen_{r,y,h} = \sum_{d} ld_{d,y,h} \qquad \forall y,h \qquad (28)$$

In constraints (18-19) and (23-24), the bilinear terms $\omega_{s,y,h}^{1} k_{s,y}^{(in)}$ and $\omega_{s,y,h}^{2} k_{s,y}^{(in)}$ are replaced by $\varsigma_{s,y,h}$ and $\kappa_{s,y,h}$, respectively (the linearization details are given in the Appendix A.1).

$$\omega_{s,y,h}^{1} DCH_{s}^{(MIN)} \leq dch_{s,y,h} \leq \varsigma_{s,y,h} \qquad \forall s,y,h \qquad (29)$$

$$\omega_{s,y,h}^{2} CH_{s}^{(MIN)} \leq ch_{s,y,h} \leq \kappa_{s,y,h} \qquad \forall s,y,h \qquad (30)$$

$$\sum_{s}(\varsigma_{s,y,h} - dch_{s,y,h}) + \sum_{s}(ch_{s,y,h} - CH_{s}^{(MIN)}) + \sum_{f}(K_{f}^{(MAX)} - gen_{f,y,h}) + \sum_{d} ld_{d,y,h} \geq PS_{y} \qquad \forall y,h \qquad (31)$$

$$\sum_s(\kappa_{s,y,h}-ch_{s,y,h})+\sum_s(dch_{s,y,h}-DCH_s^{(MIN)}) + \sum_d(D_{d,y,h}^{(MAX)}-ld_{d,y,h})+\sum_f gen_{f,y,h} \geq NS_y \quad \forall y,h \tag{32}$$

Following the discussion in Tómasson et al. (2020), the binary variables $\omega_{s,y,h}^1$ and $\omega_{s,y,h}^2$ which indicate that the PHS exists in only one of the two charging or discharging modes at any period can be relaxed in the MILP model (1)-(32). In this sense, the relaxed Linear Programming (LP) and original MILP models are interchangeable.

Consequently, the constraints associated with these binary variables (constraints (15-17) and linearization (29-32)) are removed, and constraints (18), (19), (23), and (24) are considered without binary variables. The equivalent LP model is shown below (33a-33y):

$$\begin{aligned} Maximize\ SW = \sum_y(&\sum_h\sum_d(P^{(MAX)}\,ld_{d,y,h}T) \\ &-\sum_h\sum_f(VC_f\,gen_{f,y,h}T) \\ &-\sum_h\sum_f(RC_f^{(UP)}T[K_f^{(MAX)} - gen_{f,y,h}]) \\ &-\sum_h\sum_f(RC_f^{(DN)}T[K_f^{(MAX)} - gen_{f,y,h}]) \\ &-\sum_h\sum_r(V_r gen_{r,y,h}T) \\ &-\sum_s(FC_s^{(CAP)}k_{s,y=Y}^{(in)}) \\ &-\sum_s(FC_s^{(EN)}e_{s,y}^{(in)}) \\ &-\sum_h\sum_s(RC_s^{(UP)}[k_{s,y}^{(in)} - dch_{s,y,h}]) \\ &-\sum_h\sum_s(RC_s^{(DN)}[k_{s,y}^{(in)} - ch_{s,y,h}]))/(1+i)^{y-1} \end{aligned} \tag{33a}$$

$$gen_{f,y,h} \leq K_f^{(MAX)} \quad \forall f,y,h \tag{33b}$$

$$gen_{f,y,h} - IG_f \leq RA_f \quad \forall f,y,h=1 \tag{33c}$$

$$gen_{f,y,h} - gen_{f,y,h-1} \leq RA_f \quad \forall f,y,h>1 \tag{33d}$$

$$IG_f - gen_{f,y,h} \leq RA_f \quad \forall f,y,h=1 \tag{33e}$$

$$gen_{f,y,h-1} - gen_{f,y,h} \leq RA_f \quad \forall f,y,h=1 \tag{33f}$$

$$gen_{r,y,h} \leq Q_{r,y,h}K_{r,y,h}^{(MAX)} \quad \forall r,y,h \tag{33g}$$

$$gen_{r,y,h} - IG_r \leq RA_r \quad \forall r,y,h=1 \tag{33h}$$

$$gen_{r,y,h} - gen_{r,y,h-1} \leq RA_r \quad \forall r,y,h>1 \tag{33i}$$

$$IG_r - gen_{r,y,h} \leq RA_r \quad \forall r,y,h=1 \tag{33j}$$

$$gen_{r,y,h-1} - gen_{r,y,h} \leq RA_r \quad \forall r,y,h=1 \tag{33k}$$

$$E^{(ST)} + SL_s ch_{s,y,h} - \frac{1}{SL_s}dch_{s,y,h} = e_{s,y,h}^{(st)} \quad \forall s,y,h=1 \tag{33l}$$

$$e_{s,y,h-1}^{(st)} + SL_s ch_{s,y,h} - \frac{1}{SL_s}dch_{s,y,h} = e_{s,y,h}^{(st)} \quad \forall s,y,h>1 \tag{33m}$$

$$e_{s,y,h}^{(st)} \leq e_{s,y}^{(in)} \quad \forall s,y,h \tag{33n}$$

$$DCH_s^{(MIN)} \leq dch_{s,y,h} \leq k_{s,y}^{(in)} \quad \forall s,y,h \tag{33o}$$

$$CH_s^{(MIN)} \leq ch_{s,y,h} \leq k_{s,y}^{(in)} \quad \forall s,y,h \tag{33p}$$

$$k_{s,y}^{(in)} \leq K_s^{(MAX)} \quad \forall s,y \tag{33q}$$

$$k_{s,y-1}^{(in)} \leq k_{s,y}^{(in)} \quad \forall s,y \tag{33r}$$

$$e_{s,y}^{(in)} \leq E_s^{(MAX)} \quad \forall s,y \tag{33s}$$

$$\sum_s(k_{s,y}^{(in)}-dch_{s,y,h})+\sum_s(ch_{s,y,h}-CH_s^{(MIN)}) + \sum_f(K_f^{(MAX)}-gen_{f,y,h})+\sum_d ld_{d,y,h} \geq PS_y \quad \forall y,h \tag{33t}$$

$$\sum_s(k_{s,y}^{(in)}-ch_{s,y,h})+\sum_s(dch_{s,y,h} - DCH_s^{(MIN)})+\sum_d(D_{d,y,h}^{(MAX)}-ld_{d,y,h}) + \sum_f gen_{f,y,h} \geq NS_y \quad \forall y,h \tag{33u}$$

$$ld_{d,y,h} \leq D_{d,y,h}^{(MAX)} \quad \forall d,y,h \tag{33v}$$

$$-K_l^{(MAX)} \leq flow_{l,y,h} \leq K_l^{(MAX)} \quad \forall l,y,h \tag{33w}$$

$$\sum_n\sum_s H_{l,n}A_{n,s}dch_{s,y,h} - \sum_n\sum_s H_{l,n}B_{n,s}ch_{s,y,h} + \sum_n\sum_f H_{l,n}C_{n,f}gen_{f,y,h} - \sum_n\sum_d H_{l,n}D_{n,d}ld_{d,y,h} = flow_{l,y,h} \quad \forall l,y,h \tag{33x}$$

$$\sum_f gen_{f,y,h} + \sum_s (dch_{s,y,h} - ch_{s,y,h}) + \sum_r gen_{r,y,h} = \sum_d ld_{d,y,h} \quad \forall y,h \tag{33y}$$

3. Mixed Complementarity Problem (MCP) model of PHS investment

This section introduces the MCP model, which explicitly morels various electricity-market participants. Appendix A.2 contains information on converting the LP model to the MCP model for the electricity market operator.

Constraints (34a-34b) determine the values of the charge and discharge variables

$$0 \le dch_{s,y,h} \perp \frac{-[\lambda_{y,h} - \sum_l H_{l,n} A_{n,s}(\varrho_{l,y,h} + \pi_{l,y,h})]T + \eta_{y,h} - RC_s^{(UP)}}{(1+i)^{y-1}} + \xi_{s,y,h}\frac{1}{SL_s} + \iota_{s,y,h} - \varpi_{s,y,h} \ge 0 \quad \forall s,y,h \tag{34a}$$

$$0 \le ch_{s,y,h} \perp \frac{[\lambda_{y,h} - \sum_l H_{l,n} B_{n,s}(\varrho_{l,y,h} + \pi_{l,y,h})]T + \zeta_{y,h} - RC_s^{(DN)}}{(1+i)^{y-1}} - \xi_{s,y,h} SL_s + \iota_{s,y,h} - \delta_{s,y,h} \ge 0 \quad \forall s,y,h \tag{34b}$$

The Lagrange multiplier associated with the water-balance constraints equals stored energy value:

$$\xi_{s,y,h} \text{ is Free} \perp E^{(ST)} + SL_s ch_{s,y,h} - \frac{1}{SL_s} dch_{s,y,h} = e_{s,y,h}^{(st)} \quad \forall s,y,h = 1 \tag{34c}$$

$$\xi_{s,y,h} \text{ is Free} \perp e_{s,y,h-1}^{(st)} + SL_s ch_{s,y,h} - \frac{1}{SL_s} dch_{s,y,h} = e_{s,y,h}^{(st)} \quad \forall s,y,h > 1 \tag{34d}$$

Other PHS constraints, such as capacity, are incorporated into the corresponding MCP model through controls (34e-34o):

$$0 \le k_{s,y}^{(in)} \perp \frac{\left(-\sum_h \eta_{y,h} - \sum_h \zeta_{y,h} + FC_s^{(CAP)} + RC_s^{(UP)} + RC_s^{(DN)}\right)}{(1+i)^{y-1}} - \sum_h \iota_{s,y,h} + \psi_{s,y} - \vartheta_{s,y} + \vartheta_{s,y-1} \ge 0 \quad \forall s,y \tag{34e}$$

$$0 \le e_{s,y}^{(in)} \perp \frac{FC_s^{(EN)}}{(1+i)^{y-1}} - \sum_h \mu_{s,y,h} + \nu_{s,y} \ge 0 \quad \forall s,y \tag{34f}$$

$$0 \le e_{s,y,h}^{(st)} \perp \xi_{s,y,h} + \mu_{s,y,h} \ge 0 \quad \forall s,y,h = 1 \tag{34g}$$

$$0 \le e_{s,y,h}^{(st)} \perp \xi_{s,y,h} - \xi_{s,y,h-1} + \mu_{s,y,h} \ge 0 \quad \forall s,y,h > 1 \tag{34h}$$

$$0 \le \mu_{s,y,h} \perp e_{s,y}^{(in)} - e_{s,y,h}^{(st)} \ge 0 \quad \forall s,y,h \tag{34i}$$

$$0 \le \iota_{s,y,h} \perp k_{s,y}^{(in)} - dch_{s,y,h} - ch_{s,y,h} \ge 0 \quad \forall s,y,h \tag{34j}$$

$$0 \le \varpi_{s,y,h} \perp dch_{s,y,h} - DCH_s^{(MIN)} \ge 0 \quad \forall s,y,h \tag{34k}$$

$$0 \le \delta_{s,y,h} \perp ch_{s,y,h} - CH_s^{(MIN)} \ge 0 \quad \forall s,y,h \tag{34l}$$

$$0 \le \psi_{s,y} \perp K_s^{(MAX)} - k_{s,y}^{(in)} \ge 0 \quad \forall s,y \tag{34m}$$

$$0 \le \vartheta_{s,y} \perp k_{s,y}^{(in)} - k_{s,y-1}^{(in)} \ge 0 \quad \forall s,y \tag{34n}$$

$$0 \le \nu_{s,y} \perp E_s^{(MAX)} - e_{s,y}^{(in)} \ge 0 \quad \forall s,y \tag{34o}$$

The followings are the consumption levels and load constraints:

$$0 \le ld_{d,y,h} \perp \frac{-P^{(MAX)}T}{(1+i)^{y-1}} + \tau_{d,y,h} + \lambda_{y,h} + \sum_l \sum_n \chi_{l,y,h} H_{l,n} D_{n,d} - \eta_{y,h} + \zeta_{y,h} \ge 0 \quad \forall d,y,h \tag{34p}$$

$$0 \le \tau_{d,y,h} \perp D_{d,y,h}^{(MAX)} - ld_{d,y,h} \ge 0 \quad \forall d,y,h \tag{34q}$$

The capacity and production constraints of conventional generators and renewable technologies are expressed as follows:

$$0 \le gen_{f,y,h} \perp \frac{\left(VC_f T - RC_f^{(UP)} T - RC_f^{(DN)} T\right)}{(1+i)^{y-1}} + \alpha_{f,y,h} - \lambda_{y,h} - \sum_l \sum_n \chi_{l,y,h} H_{l,n} C_{n,f} + \eta_{y,h} - \zeta_{y,h} + \phi_{f,y,h}^{(1)} - \phi_{f,y,h+1}^{(1)} - \phi_{f,y,h}^{(2)} + \phi_{f,y,h+1}^{(2)} \ge 0 \quad \forall f,y,h \tag{34r}$$

$$0 \le \alpha_{f,y,h} \perp K_f^{(MAX)} - gen_{f,y,h} \ge 0 \quad \forall f,y,h \tag{34s}$$

$$0 \le gen_{r,y,h} \perp \frac{V_r T}{(1+i)^{y-1}} + \beta_{r,y,h} - \lambda_{y,h} + \phi_{r,y,h}^{(1)} - \phi_{r,y,h+1}^{(1)} - \phi_{r,y,h}^{(2)} + \phi_{r,y,h+1}^{(2)} \ge 0 \quad \forall r,y,h \tag{34t}$$

$$0 \le \beta_{r,y,h} \perp Q_{r,y,h} K_{r,y,h}^{(MAX)} - gen_{r,y,h} \ge 0 \quad \forall r,y,h \tag{34u}$$

The Lagrange multiplier associated with the electrical-energy balance constraint in the proposed MCP model indicates the energy price, which is given below:

$$\lambda_{y,h} \text{ is Free} \perp \sum_f gen_{f,y,h} + \sum_s (dch_{s,y,h} - ch_{s,y,h}) + \sum_r gen_{r,y,h} = \sum_d ld_{d,y,h} \quad \forall y,h \tag{34v}$$

Constraints (34w-34z) describe constraints related to the flow of lines in the MCP model:

$$0 \le \varrho_{l,y,h} \perp flow_{l,y,h} + K_l^{(MAX)} \ge 0 \quad \forall l,y,h \tag{34w}$$

$$0 \le \pi_{l,y,h} \perp K_l^{(MAX)} - flow_{l,y,h} \ge 0 \quad \forall l,y,h \tag{34x}$$

$$0 \le flow_{l,y,h} \perp -[\lambda_{y,h} - \sum_l H_{l,n^{(ter)}} (\varrho_{l,y,h} + \pi_{l,y,h})] + [\lambda_{y,h} - \sum_l H_{l,n^{(org)}} (\varrho_{l,y,h} + \pi_{l,y,h})] - \varrho_{l,y,h} + \pi_{l,y,h} + \chi_{l,y,h} \ge 0 \quad \forall l,y,h \tag{34y}$$

$$\chi_{l,y,h}\ is\ Free \perp \sum_n \sum_s H_{l,n} A_{n,s} dch_{s,y,h} - \sum_n \sum_s H_{l,n} B_{n,s} ch_{s,y,h} + \sum_n \sum_f H_{l,n} C_{n,f} gen_{f,y,h} - \sum_n \sum_d H_{l,n} D_{n,d} ld_{d,y,h} = flow_{l,y,h} \quad \forall l,y,h \tag{34z}$$

Frequency control services, which are one of the features of PHSS, are considered in the MCP model as follows:

$$0 \le \eta_{y,h} \perp \sum_s (k_{s,y}^{(in)} - dch_{s,y,h}) + \sum_s (ch_{s,y,h} - CH_s^{(MIN)}) + \sum_f (K_f^{(MAX)} - gen_{f,y,h}) + \sum_d ld_{d,y,h} - PS_y \ge 0 \quad \forall y,h \tag{34aa}$$

$$0 \le \zeta_{y,h} \perp \sum_s (k_{s,y}^{(in)} - ch_{s,y,h}) + \sum_s (dch_{s,y,h} - DCH_s^{(MIN)}) + \sum_d (D_{d,y,h}^{(MAX)} - ld_{d,y,h}) + \sum_f gen_{f,y,h} - NS_y \ge 0 \quad \forall y,h \tag{34bb}$$

The MCP model's up and down ramping limits for each conventional generator are presented below. In these constraints, the $\phi_{f,y,h}^{(1)}$ and $\phi_{f,y,h}^{(2)}$ variables are considered as the corresponding Lagrange coefficients:

$$0 \le \phi_{f,y,h}^{(1)} \perp RA_f - gen_{f,y,h} + IG_f \ge 0 \quad \forall f,y,h = 1 \tag{34cc}$$

$$0 \le \phi_{f,y,h}^{(1)} \perp RA_f - gen_{f,y,h} + gen_{f,y,h-1} \ge 0 \quad \forall f,y,h > 1 \tag{34dd}$$

$$0 \le \phi_{f,y,h}^{(2)} \perp RA_f - IG_f + gen_{f,y,h} \ge 0 \quad \forall f,y,h = 1 \tag{34ee}$$

$$0 \le \phi_{f,y,h}^{(2)} \perp RA_f - gen_{f,y,h-1} + gen_{f,y,h} \ge 0 \quad \forall f,y,h > 1 \tag{33ff}$$

As previously stated, the constraints (34gg-34jj), with the $\phi_{r,y,h}^{(1)}$ and $\phi_{r,y,h}^{(2)}$ variables as Lagrange coefficients, represent the up and down ramping limits of renewable technology in our proposed MCP model:

$$0 \le \phi_{r,y,h}^{(1)} \perp RA_r - gen_{r,y,h} + IG_r \ge 0 \quad \forall r,y,h = 1 \tag{34gg}$$

$$0 \le \phi_{r,y,h}^{(1)} \perp RA_r - gen_{r,y,h} + gen_{r,y,h-1} \ge 0 \quad \forall r,y,h > 1 \tag{34hh}$$

$$0 \le \phi_{r,y,h}^{(2)} \perp RA_r - IG_r + gen_{r,y,h} \ge 0 \quad \forall r,y,h = 1 \tag{34ii}$$

$$0 \le \phi_{r,y,h}^{(2)} \perp RA_r - gen_{r,y,h-1} + gen_{r,y,h} \ge 0 \quad \forall r,y,h > 1 \tag{34jj}$$

The developed MCP adds a combinatorial screw to the classic square system of nonlinear equations. In its most basic form, the combinatorial problem is to choose a subset of n from $2n$ inequalities that will satisfy as equations (Ferris and T. S. Munson, 2000). MCP models, such as the one presented in this paper, are computationally expensive. In the following section, we propose Benders decomposition to solve our MCP model.

4. The Benders decomposition for the MCP model

The MILP problems are optimization problems in which some variables take continuous variables and some only integer values, so they are computationally hard problems. Benders proposed the decomposition technique to solve these problems in 1962 (Murphy, 2013). Benders decomposition technique divided the main problem into a pure Integer Programming (IP) problem and a pure LP problem, which were solved repeatedly until a general solution was obtained. The IP problem is referred to as the Master Problem (MP), to which Benders cuts are added, and the LP problem is called the Sub Problem (SP), from which the Benders cuts are generated. The advantage of this method is that solving two sub-problems is more straightforward than solving the main problem, though it may be necessary to solve them several times (Murphy, 2013). Appendix B summarizes the Benders decomposition technique. Fig. 1 depicts the Benders decomposition algorithm (Kalvelagen, 2002). Section 4.1 contains information on the MP and SP of the Benders decomposition for the MCP model.

4.1. The Benders decomposition for the MCP model

Applying the complementary slackness conditions in the MCP model necessitates using binary variables ($\theta_{s,y,h}^1, \theta_{s,y,h}^2, \dots, \theta_{f,y,h}^{19}$) (In this case, the binary variables $\theta_{s,y,h}^1, \theta_{s,y,h}^2, \dots, \theta_{f,y,h}^{19}$ are fixed, with the resulting problem being an LP model). The SP duality for the MCP problem is expressed as follows:

$$\textbf{SP:} Min\ \sum_s \sum_y \sum_h RC_s^{(UP)} u_{s,y,h}^1 + \sum_s \sum_y \sum_h RC_s^{(DN)} u_{s,y,h}^2 - \sum_s \sum_y (FC_s^{(CAP)} + RC_s^{(UP)} + RC_s^{(DN)}) u_{s,y}^{11} - \sum_s \sum_y FC_s^{(EN)} u_{s,y}^{12} - \sum_s \sum_y E^{(ST)} u_{s,y,h=1}^5 + \sum_s \sum_y \sum_h DCH_s^{(MIN)} u_{s,y,h}^9 + \sum_s \sum_y \sum_h CH_s^{(MIN)} u_{s,y,h}^{10} - \sum_s \sum_y K_s^{(MAX)} u_{s,y}^{13} - \sum_s \sum_y E_s^{(MAX)} u_{s,y}^{15} - \sum_f [\sum_y \sum_h (VC_f - RC_f^{(UP)} - RC_f^{(DN)}) Tv_{f,y,h}^1]/(1+i)^{y-1} - \tag{35a}$$

$\sum_f \sum_y \sum_h K_f^{(MAX)} v_{f,y,h}^2 - \sum_f \sum_y \sum_{h=1} (RA_f +$
$IG_f) v_{f,y,}^3 - \sum_f \sum_y \sum_{h>1} RA_f v_{f,y,h}^4 -$
$\sum_f \sum_y \sum_{h=1} (RA_f - IG_f) v_{f,y,h}^5 -$
$\sum_f \sum_y \sum_{h>1} RA_f v_{f,y,h}^6 +$
$\sum_d [\sum_y \sum_h P^{(MAX)} T v_{d,y,h}^7] / (1+i)^{y-1} -$
$\sum_d \sum_y \sum_h D_{d,y,h}^{(MAX)} v_{d,y,h}^8 -$
$\sum_r [\sum_y \sum_h V_r T v_{r,y,h}^9] / (1+i)^{y-1} -$
$\sum_r \sum_y \sum_h Q_{r,y,h} K_{r,y,h}^{(MAX)} v_{r,y,h}^{10} -$
$\sum_r \sum_y \sum_{h=1} (RA_r + IG_r) v_{r,y,h}^{11} -$
$\sum_r \sum_y \sum_{h>1} RA_r v_{r,y,h}^{12} - \sum_r \sum_y \sum_{h=1} (RA_r -$
$IG_r) v_{r,y,h}^{13} - \sum_r \sum_y \sum_{h>1} RA_r v_{r,y,h}^{14} -$
$\sum_l \sum_y \sum_h K_l^{(MAX)} (w_{l,y,h}^1 + w_{l,y,h}^2) +$
$\sum_s \sum_f \sum_y \sum_h (CH_s^{(MIN)} - K_f^{(MAX)} +$
$PS_y) w_{y,h}^6 + \sum_s \sum_d \sum_y \sum_h (DCH_s^{(MIN)} -$
$D_{d,y,h}^{(MAX)} + NS_y) w_{y,h}^7 -$
$\sum_s \sum_y \sum_h \theta_{s,y,h}^1 M u_{s,y,h}^{16} - \sum_s \sum_y \sum_h ((1-$
$\theta_{s,y,h}^1) M + RC_s^{(UP)}) u_{s,y,h}^{17} -$
$\sum_s \sum_y \sum_h \theta_{s,y,h}^2 M u_{s,y,h}^{18} - \sum_s \sum_y \sum_h ((1-$
$\theta_{s,y,h}^2) M + RC_s^{(DN)}) u_{s,y,h}^{19} -$
$\sum_s \sum_y \theta_{s,y,h=1}^3 M u_{s,y,h=1}^{20} - \sum_s \sum_y (1-$
$\theta_{s,y,h=1}^3) M u_{s,y,h=1}^{21} -$
$\sum_s \sum_y \sum_{h>1} \theta_{s,y,h}^4 M u_{s,y,h}^{22} - \sum_s \sum_y \sum_{h>1} (1-$
$\theta_{s,y,h}^4) M u_{s,y,h}^{23} - \sum_s \sum_y \sum_h \theta_{s,y,h}^5 M u_{s,y,h}^{24} -$
$\sum_s \sum_y \sum_h (1-\theta_{s,y,h}^5) M u_{s,y,h}^{25} -$
$\sum_s \sum_y \sum_h \theta_{s,y,h}^6 M u_{s,y,h}^{26} - \sum_s \sum_y \sum_h (1-$
$\theta_{s,y,h}^6) M u_{s,y,h}^{27} - \sum_s \sum_y \sum_h \theta_{s,y,h}^7 M u_{s,y,h}^{28} -$
$\sum_s \sum_y \sum_h ((1-\theta_{s,y,h}^7) M + DCH_s^{(MIN)}) u_{s,y,h}^{29} -$
$\sum_s \sum_y \sum_h \theta_{s,y,h}^8 M u_{s,y,h}^{30} - \sum_s \sum_y \sum_h ((1-$
$\theta_{s,y,h}^8) M + CH_s^{(MIN)}) u_{s,y,h}^{31} - \sum_s \theta_{s,y}^9 M u_{s,y}^{32} -$
$\sum_s \sum_y ((1-\theta_{s,y}^9) M - FC_s^{(CAP)} - RC_s^{(UP)} -$
$RC_s^{(DN)}) u_{s,y}^{33} - \sum_s \theta_{s,y}^{10} M u_{s,y}^{34} - \sum_s \sum_y ((1-$
$\theta_{s,y}^{10}) M - FC_s^{(EN)}) u_{s,y}^{35} - \sum_s \theta_{s,y}^{11} M u_{s,y}^{36} -$
$\sum_s \sum_y ((1-\theta_{s,y}^{11}) M - K_s^{(MAX)}) u_{s,y}^{37} -$
$\sum_s \theta_{s,y}^{12} M u_{s,y}^{38} - \sum_s \sum_y (1-\theta_{s,y}^{12}) M u_{s,y}^{39} -$
$\sum_s \theta_{s,y}^{13} M u_{s,y}^{40} - \sum_s \sum_y ((1-\theta_{s,y}^{13}) M -$
$E_s^{(MAX)}) u_{s,y}^{41} - \sum_f \sum_y \sum_h \theta_{f,y,h}^{14} M v_{f,y,h}^{15} -$
$\sum_f [\sum_y \sum_h ((1-\theta_{f,y,h}^{14}) M - VC_f T +$
$RC_f^{(UP)} T + RC_f^{(DN)} T) v_{f,y,h}^{16}] / (1+i)^{y-1} -$
$\sum_f \sum_y \sum_h \theta_{f,y,h}^{15} M v_{f,y,h}^{17} - \sum_f \sum_y \sum_h ((1-$
$\theta_{f,y,h}^{15}) M - K_f^{(MAX)}) v_{f,y,h}^{18} -$
$\sum_f \sum_y \theta_{f,y,h=1}^{16} M v_{f,y,h=1}^{19} - \sum_f \sum_y ((1-$
$\theta_{f,y,h=1}^{16}) - RA_f - IG_f) M v_{f,y,h=1}^{20} -$
$\sum_f \sum_y \sum_{h>1} \theta_{f,y,h}^{17} M v_{f,y,h}^{21} - \sum_f \sum_y \sum_{h>1} ((1-$
$\theta_{f,y,h}^{17}) M - RA_f) v_{f,y,h}^{22} -$
$\sum_f \sum_y \theta_{f,y,h=1}^{18} M v_{f,y,h=1}^{23} - \sum_f \sum_y ((1-$
$\theta_{f,y,h=1}^{18}) - RA_f + IG_f) M v_{f,y,h=1}^{24} -$
$\sum_f \sum_y \sum_{h>1} \theta_{f,y,h}^{19} M v_{f,y,h}^{25} - \sum_f \sum_y \sum_{h>1} ((1-$
$\theta_{f,y,h}^{19}) M - RA_f) v_{f,y,h}^{26} -$
$\sum_d \sum_y \sum_h \theta_{d,y,h}^{20} M v_{d,y,h}^{27} - \sum_d [\sum_y \sum_h ((1-$
$\theta_{d,y,h}^{20}) M + P^{(MAX)} T) v_{d,y,h}^{28}] / (1+i)^{y-1} -$
$\sum_d \sum_y \sum_h \theta_{d,y,h}^{21} M v_{d,y,h}^{29} - \sum_d \sum_y \sum_h ((1-$
$\theta_{d,y,h}^{221}) M - D_{d,y,h}^{(MAX)}) v_{d,y,h}^{30} -$
$\sum_r \sum_y \sum_h \theta_{r,y,h}^{22} M v_{r,y,h}^{31} - \sum_r [\sum_y \sum_h ((1-$
$\theta_{r,y,h}^{22}) M - V_r T) v_{r,y,h}^{32}] / (1+i)^{y-1} -$
$\sum_r \sum_y \sum_h \theta_{r,y,h}^{23} M v_{r,y,h}^{33} - \sum_r \sum_y \sum_h ((1-$
$\theta_{r,y,h}^{23}) M - Q_{r,y,h} K_{r,y,h}^{(MAX)}) v_{r,y,h}^{34} -$
$\sum_f \sum_y \theta_{f,y,h=1}^{24} M v_{r,y,h=1}^{35}$

Subject to: $\frac{\sum_s(\sum_l \sum_n H_{l,n} A_{n,s}) T u_{s,y,h}^1}{(1+i)^{y-1}} -$ (35b)
$\frac{\sum_s(\sum_l \sum_n H_{l,n} B_{n,s}) T u_{s,y,h}^2}{(1+i)^{y-1}} +$
$\sum_f (\sum_l \sum_n H_{l,n} C_{n,f}) v_{f,y,h}^1 -$
$\sum_d (\sum_l \sum_n H_{l,n} D_{n,d}) v_{d,y,h}^7 +$
$[\sum_n H_{l,n} E_{n,l-} \sum_n H_{l,n} F_{n,l} - 1] w_{l,y,h}^4 -$
$\frac{\sum_s(\sum_l \sum_n H_{l,n} A_{n,s}) T u_{s,y,h}^{17}}{(1+i)^{y-1}} + \frac{\sum_s(\sum_l \sum_n H_{l,n} B_{n,s}) T u_{s,y,h}^{19}}{(1+i)^{y-1}} -$
$\sum_f (\sum_l \sum_n H_{l,n} C_{n,f}) v_{f,y,h}^{16} +$
$\sum_d (\sum_l \sum_n H_{l,n} D_{n,d}) v_{d,y,h}^{28} -$
$[\sum_n H_{l,n} E_{n,l-} \sum_n H_{l,n} F_{n,l} - 1] w_{l,y,h}^{13} - w_{l,y,h}^8 \le$
$0 \quad \forall l, y, h$

$\frac{\sum_s(\sum_l \sum_n H_{l,n} A_{n,s}) T u_{s,y,h}^1}{(1+i)^{y-1}} - \frac{\sum_s(\sum_l \sum_n H_{l,n} B_{n,s}) T u_{s,y,h}^2}{(1+i)^{y-1}} +$ (35c)
$\sum_f (\sum_l \sum_n H_{l,n} C_{n,f}) v_{f,y,h}^1 -$
$\sum_d (\sum_l \sum_n H_{l,n} D_{n,d}) v_{d,y,h}^7 +$
$[\sum_n H_{l,n} E_{n,l-} \sum_n H_{l,n} F_{n,l} + 1] w_{l,y,h}^4 -$
$\frac{\sum_s(\sum_l \sum_n H_{l,n} A_{n,s}) T u_{s,y,h}^{17}}{(1+i)^{y-1}} + \frac{\sum_s(\sum_l \sum_n H_{l,n} B_{n,s}) T u_{s,y,h}^{19}}{(1+i)^{y-1}} -$
$\sum_f (\sum_l \sum_n H_{l,n} C_{n,f}) v_{f,y,h}^{16} +$
$\sum_d (\sum_l \sum_n H_{l,n} D_{n,d}) v_{d,y,h}^{28} -$
$[\sum_n H_{l,n} E_{n,l-} \sum_n H_{l,n} F_{n,l} + 1] w_{l,y,h}^{13} - w_{l,y,h}^{10} \le$
$0 \quad \forall l, y, h$

$\frac{\sum_s u_{s,y,h}^1}{(1+i)^{y-1}} - u_{s,y}^{11} - \frac{\sum_s u_{s,y,h}^{17}}{(1+i)^{y-1}} - u_{s,y}^{33} + \sum_f (v_{f,y,h}^1 -$ (35d)
$v_{f,y,h}^{16}) - \sum_d (v_{d,y,h}^7 - v_{d,y,h}^{28}) - w_{y,h}^6 \le$
$0 \quad \forall y, h$

$u_{s,y,h}^1 + u_{s,y,h}^2 - u_{s,y}^{11} - u_{s,y,h}^{17} - u_{s,y,h}^{19} - u_{s,y}^{33}$
$- u_{s,y,h}^{26} \le 0 \quad \forall s, y, h$ (35e)

$-u_{s,y,h}^1 + u_{s,y,h}^{17} - u_{s,y,h}^{28} \le 0 \quad \forall s, y, h$ (35f)

$\frac{\sum_s u_{s,y,h}^2}{(1+i)^{y-1}} - u_{s,y}^{11} - \frac{\sum_s u_{s,y,h}^{19}}{(1+i)^{y-1}} + u_{s,y}^{34} - \sum_f (v_{f,y,h}^1 -$
$v_{f,y,h}^{16}) + \sum_d (v_{d,y,h}^7 - v_{d,y,h}^{28}) - w_{y,h}^7 \le$ (35g)
$0 \quad \forall y, h$

$-u_{s,y,h}^2 + u_{s,y,h}^{19} - u_{s,y,h}^{30} \le 0 \quad \forall s, y, h$ (35h)

$u_{s,y}^{11} - u_{s,y}^{33} - u_{s,y}^{36} \le 0 \quad \forall s, y$ (35i)

$u_{s,y}^{12} - u_{s,y}^{35} - u_{s,y}^{40} \le 0 \quad \forall s, y$ (35j)

$-u_{s,y}^{11} + u_{s,y-1}^{11} + u_{s,y}^{33} - u_{s,y-1}^{33} - u_{s,y}^{38}$
$\le 0 \quad \forall s, y$ (35k)

$$(u^5_{s,y,h})_{|h=1}SL_s + (u^6_{s,y,h})_{|h>1}SL_s - u^8_{s,y,h} + u^{10}_{s,y,h} - \sum_l\sum_n H_{l,n}B_{n,s}w^3_{l,y,h} - w^5_{y,h} + w^6_{y,h} - w^7_{y,h} - u^{18}_{s,y,h} + u^{27}_{s,y,h} - u^{31}_{s,y,h} - w^{15}_{y,h} + w^{17}_{y,h} \le 0 \quad \forall s,y,h \tag{35l}$$

$$-\frac{(u^5_{s,y,h})_{|h=1}}{SL_s} + \frac{(u^6_{s,y,h})_{|h>1}}{SL_s} - u^8_{s,y,h} + u^9_{s,y,h} + \sum_l\sum_n H_{l,n}A_{n,s}w^3_{l,y,h} + w^5_{y,h} - w^6_{y,h} + w^7_{y,h} - u^{16}_{s,y,h} + u^{27}_{s,y,h} - u^{29}_{s,y,h} + w^{15}_{y,h} - w^{17}_{y,h} \le 0 \quad \forall s,y,h \tag{35m}$$

$$-(u^5_{s,y,h})_{|h=1} + (u^6_{s,y,h-1})_{|h>1} - (u^6_{s,y,h})_{|h>1} - u^7_{s,y,h} - (u^{20}_{s,y,h})_{|h=1} - (u^{22}_{s,y,h})_{|h>1} + u^{25}_{s,y,h} \le 0 \quad \forall s,y,h \tag{35n}$$

$$\sum_h (u^7_{s,y,h} - u^{25}_{s,y,h}) - u^{14}_{s,y} - u^{34}_{s,y} + u^{41}_{s,y} \le 0 \quad \forall s,y \tag{35o}$$

$$\sum_h (u^8_{s,y,h} - u^{27}_{s,y,h}) - u^{13}_{s,y} + u^{14}_{s,y} - u^{14}_{s,y-1} - u^{32}_{s,y} + u^{37}_{s,y} - u^{39}_{s,y} + u^{39}_{s,y-1} + \sum_h (w^6_{y,h} + w^7_{y,h} - w^{15}_{y,h} - w^{17}_{y,h}) \le 0 \quad \forall s,y \tag{35p}$$

$$v^1_{f,y,h} - v^{16}_{f,y,h} - v^{17}_{f,y,h} \le 0 \quad \forall f,y,h \tag{35q}$$

$$v^1_{f,y,h} - v^1_{f,y,h+1} - v^{16}_{f,y,h} + v^{16}_{f,y,h+1} - (v^{19}_{f,y,h})_{|h=1} - (v^{21}_{f,y,h})_{|h>1} \le 0 \quad \forall f,y,h \tag{35r}$$

$$-v^1_{f,y,h} + v^1_{f,y,h+1} + v^{16}_{f,y,h} - v^{16}_{f,y,h+1} - (v^{23}_{f,y,h})_{|h=1} - (v^{25}_{f,y,h})_{|h>1} \le 0 \quad \forall f,y,h \tag{35s}$$

$$-v^2_{f,y,h} - \left(v^3_{f,y,h}\right)_{|h=1} - \left(v^4_{f,y,h} - v^4_{f,y,h-1}\right)_{|h>1} + \left(v^5_{f,y,h}\right)_{|h=1} - \left(v^6_{f,y,h-1} - v^6_{f,y,h}\right)_{|h>1} + \sum_l\sum_n H_{l,n}C_{n,f}w^3_{l,y,h} + w^5_{y,h} - w^6_{y,h} + w^7_{y,h} - v^{18}_{f,y,h} + \left(v^{20}_{f,y,h}\right)_{|h=1} + \left(v^{22}_{f,y,h} - v^{22}_{f,y,h-1}\right)_{|h>1} - \left(v^{24}_{f,y,h}\right)_{|h=1} + \left(v^{26}_{f,y,h-1} - v^{26}_{f,y,h}\right)_{|h>1} + w^{15}_{y,h} - w^{17}_{y,h} \le 0 \quad \forall f,y,h \tag{35t}$$

$$v^7_{d,y,h} - v^{28}_{d,y,h} - v^{29}_{d,y,h} \le 0 \quad \forall d,y,h \tag{35u}$$

$$-v^8_{d,y,h} - \sum_l\sum_n H_{l,n}D_{n,d}w^3_{l,y,h} - w^5_{y,h} + w^6_{y,h} - w^7_{y,h} - v^{27}_{d,y,h} + v^{30}_{d,y,h} - w^{15}_{y,h} + w^{17}_{y,h} \le 0 \quad \forall d,y,h \tag{35v}$$

$$v^9_{r,y,h} - v^{32}_{r,y,h} - v^{33}_{r,y,h} \le 0 \quad \forall r,y,h \tag{35w}$$

$$v^9_{r,y,h} - v^9_{r,y,h+1} - v^{32}_{r,y,h} + v^{32}_{r,y,h+1} - (v^{35}_{r,y,h})_{|h=1} - (v^{37}_{r,y,h})_{|h>1} \le 0 \quad \forall r,y,h \tag{35x}$$

$$-v^9_{r,y,h} + v^9_{r,y,h+1} + v^{32}_{r,y,h} - v^{32}_{r,y,h+1} - (v^{39}_{r,y,h})_{|h=1} - (v^{41}_{r,y,h})_{|h>1} \le 0 \quad \forall r,y,h \tag{35y}$$

$$-v^{10}_{r,y,h} - \left(v^{11}_{r,y,h}\right)_{|h=1} - \left(v^{12}_{r,y,h} - v^{12}_{r,y,h-1}\right)_{|h>1} + \left(v^{13}_{r,y,h}\right)_{|h=1} - \left(v^{14}_{r,y,h-1} - v^{14}_{r,y,h}\right)_{|h>1} + w^5_{y,h} - v^{31}_{r,y,h} + v^{34}_{r,y,h} + \left(v^{36}_{r,y,h}\right)_{|h=1} + \left(v^{38}_{r,y,h} - v^{38}_{r,y,h-1}\right)_{|h>1} - \left(v^{40}_{r,y,h}\right)_{|h=1} + \left(v^{42}_{r,y,h-1} - v^{42}_{r,y,h}\right)_{|h>1} \le 0 \quad \forall r,y,h \tag{35z}$$

$$w^1_{l,y,h} - w^2_{l,y,h} - w^3_{l,y,h} - w^9_{l,y,h} + w^{11}_{l,y,h} - w^{12}_{l,y,h} \le 0 \quad \forall l,y,h \tag{35aa}$$

$$\sum_s \frac{(-u^1_{s,y,h}T)}{(1+i)^{y-1}} + \frac{(u^2_{s,y,h}T)}{(1+i)^{y-1}} + \frac{(u^{17}_{s,y,h}T)}{(1+i)^{y-1}} - \frac{(u^{19}_{s,y,h}T)}{(1+i)^{y-1}} + \sum_f(-v^1_{f,y,h} + v^{16}_{f,y,h}) + \sum_d(v^7_{d,y,h} - v^{28}_{d,y,h}) + \sum_r(-v^9_{r,y,h} + v^{32}_{r,y,h}) \le 0 \quad \forall y,h \tag{35bb}$$

$$\frac{u^1_{s,y,h}}{SL_s} - \frac{u^2_{s,y,h}}{SL_s} + \left(u^3_{s,y,h}\right)_{|h=1} + \left(u^4_{s,y,h} - u^4_{s,y,h-1}\right)_{|h>1} - \frac{u^{17}_{s,y,h}}{SL_s} + \frac{u^{19}_{s,y,h}}{SL_s} - \left(u^{21}_{s,y,h}\right)_{|h=1} - \left(u^{23}_{s,y,h} - u^{23}_{s,y,h-1}\right)_{|h>1} \le 0 \quad \forall s,y,h \tag{35cc}$$

$$-\sum_n\sum_f H_{l,n}C_{n,f}v^1_{f,y,h} + \sum_n\sum_d H_{l,n}D_{n,d}v^7_{d,y,h} + w^4_{l,y,h} + \sum_n\sum_f H_{l,n}C_{n,f}v^{16}_{f,y,h} - \sum_n\sum_d H_{l,n}D_{n,d}v^{28}_{d,y,h} - w^{13}_{l,y,h} \le 0 \quad \forall l,y,h \tag{35dd}$$

$$u, v, w \ge 0 \qquad (the\ dual\ variables) \tag{35ee}$$

$$\theta = \overline{\theta} \tag{35ff}$$

The solution in the MP moves toward optimal values by producing cutting planes in the direction of hard variables convergence. The MP has the role of leader, and the SP has the follower role. The MP related to the MCP problem is presented below:

$$\text{MP:} \quad Maximize\ Z \tag{36a}$$

Subject to:
$$Z \le \sum_s\sum_y\sum_h RC^{(UP)}_s u^1_{s,y,h} + \sum_s\sum_y\sum_h RC^{(DN)}_s u^2_{s,y,h} - \sum_s\sum_y (FC^{(CAP)}_s + RC^{(UP)}_s + RC^{(DN)}_s) u^{11}_{s,y} - \sum_s\sum_y FC^{(EN)}_s u^{12}_{s,y} - \sum_s\sum_y E^{(ST)} u^5_{s,y,h=1} + \sum_s\sum_y\sum_h DCH^{(MIN)}_s u^9_{s,y,h} + \sum_s\sum_y\sum_h CH^{(MIN)}_s u^{10}_{s,y,h} - \sum_s\sum_y K^{(MAX)}_s u^{13}_{s,y} - \sum_s\sum_y E^{(MAX)}_s u^{15}_{s,y} - \sum_f [\sum_y\sum_h (VC_f - RC^{(UP)}_f - RC^{(DN)}_f) T v^1_{f,y,h}]/(1+i)^{y-1} - \sum_f\sum_y\sum_h K^{(MAX)}_f v^2_{f,y,h} - \sum_f\sum_y\sum_{h=1} \left(RA_f + IG_f\right) v^3_{f,y,h} - \sum_f\sum_y\sum_{h>1} RA_f v^4_{f,y,h} - \sum_f\sum_y\sum_{h=1}\left(RA_f - IG_f\right) v^5_{f,y,h} - \sum_f\sum_y\sum_{h>1} RA_f v^6_{f,y,h} + \sum_d [\sum_y\sum_h P^{(MAX)} T v^7_{d,y,h}]/(1+i)^{y-1} - \sum_d\sum_y\sum_h D^{(MAX)}_{d,y,h} v^8_{d,y,h} - \sum_r [\sum_y\sum_h V_r T v^9_{r,y,h}]/(1+i)^{y-1} - \sum_r\sum_y\sum_h Q_{r,y,h} K^{(MAX)}_{r,y,h} v^{10}_{r,y,h} - \sum_r\sum_y\sum_{h=1}(RA_r + IG_r) v^{11}_{r,y,h} - \sum_r\sum_y\sum_{h>1} RA_r v^{12}_{r,y,h} - \sum_r\sum_y\sum_{h=1}(RA_r - IG_r) v^{13}_{r,y,h} - \sum_r\sum_y\sum_{h>1} RA_r v^{14}_{r,y,h} - \sum_l\sum_y\sum_h K^{(MAX)}_l \left(w^1_{l,y,h} + w^2_{l,y,h}\right) + \sum_s\sum_f\sum_y\sum_h \left(CH^{(MIN)}_s - K^{(MAX)}_f + PS_y\right) w^6_{y,h} + \sum_s\sum_d\sum_y\sum_h \left(DCH^{(MIN)}_s - D^{(MAX)}_{d,y,h} + NS_y\right) w^7_{y,h} + \sum_s\sum_y\sum_h [-M u^{16}_{s,y,h} - (M + RC^{(UP)}_s) u^{17}_{s,y,h}] \theta^1_{s,y,h} + \sum_s\sum_y\sum_h [-M u^{18}_{s,y,h} - (M + RC^{(DN)}_s) u^{19}_{s,y,h}] \theta^2_{s,y,h} + \sum_s\sum_y\sum_{h=1} [-M u^{20}_{s,y,h} - M u^{21}_{s,y,h}] \theta^3_{s,y,h} + \sum_s\sum_y\sum_{h>1} [-M u^{22}_{s,y,h} - M u^{23}_{s,y,h}] \theta^4_{s,y,h} + \sum_s\sum_y\sum_h [-M u^{24}_{s,y,h} - M u^{25}_{s,y,h}] \theta^5_{s,y,h} + \tag{36b}$$

$\sum_s \sum_y \sum_h[-Mu^{26}_{s,y,h} - Mu^{27}_{s,y,h}]\theta^{6}_{s,y,h} +$
$\sum_s \sum_y \sum_h[-Mu^{28}_{s,y,h} -$
$\left(M + DCH_s^{(MIN)}\right)u^{29}_{s,y,h}]\theta^{7}_{s,y,h} +$
$\sum_s \sum_y \sum_h[-Mu^{30}_{s,y,h} -$
$\left(M + CH_s^{(MIN)}\right)u^{31}_{s,y,h}]\theta^{8}_{s,y,h} + \sum_s \sum_y[-Mu^{32}_{s,y} -$
$\left(M - FC_s^{(CAP)} - RC_s^{(UP)} - RC_s^{(DN)}\right)u^{33}_{s,y}]\theta^{9}_{s,y} +$
$\sum_s \sum_y[-Mu^{34}_{s,y} - \left(M - FC_s^{(EN)}\right)u^{35}_{s,y}]\theta^{10}_{s,y} +$
$\sum_s \sum_y[-Mu^{36}_{s,y} - \left(M - K_s^{(MAX)}\right)u^{37}_{s,y}]\theta^{11}_{s,y} +$
$\sum_s \sum_y[-Mu^{38}_{s,y} - Mu^{39}_{s,y}]\theta^{12}_{s,y} + \sum_s \sum_y[-Mu^{40}_{s,y} -$
$\left(M - E_s^{(MAX)}\right)u^{41}_{s,y}]\theta^{13}_{s,y} + \sum_f \sum_y \sum_h[-Mv^{15}_{f,y,h} -$
$\frac{\left(M-(VC_f-RC_f^{(UP)}-RC_f^{(DN)})T\right)}{(1+i)^{y-1}} v^{16}_{f,y,h}]\theta^{14}_{f,y,h} +$
$\sum_f \sum_y \sum_h[-Mv^{17}_{f,y,h} -$
$\left(M - K_f^{(MAX)}\right)v^{18}_{f,y,h}]\theta^{15}_{f,y,h} +$
$\sum_f \sum_y \sum_{h=1}[-Mv^{19}_{f,y,h} - \left(M - RA_f -\right.$
$\left.IG_f\right)v^{20}_{f,y,h}]\theta^{16}_{f,y,h} + \sum_f \sum_y \sum_{h>1}[-Mv^{21}_{f,y,h} -$
$\left(M - RA_f\right)v^{22}_{f,y,h}]\theta^{17}_{f,y,h} +$
$\sum_f \sum_y \sum_{h=1}[-Mv^{23}_{f,y,h} - \left(M - RA_f +\right.$
$\left.IG_f\right)v^{24}_{f,y,h}]\theta^{18}_{f,y,h} + \sum_f \sum_y \sum_{h>1}[-Mv^{25}_{f,y,h} -$
$\left(M - RA_f\right)v^{26}_{f,y,h}]\theta^{19}_{f,y,h} + \sum_d \sum_y \sum_h[-Mv^{27}_{d,y,h} -$
$\frac{(M+P^{(MAX)}T)}{(1+i)^{y-1}} v^{28}_{d,y,h}]\theta^{20}_{d,y,h} + \sum_d \sum_y \sum_h[-Mv^{29}_{d,y,h} -$
$\left(M - D_{d,y,h}^{(MAX)}\right)v^{30}_{d,y,h}]\theta^{21}_{d,y,h} +$
$\sum_r \sum_y \sum_h[-Mv^{31}_{r,y,h} - \frac{(M-V_rT)}{(1+i)^{y-1}} v^{32}_{r,y,h}]\theta^{22}_{r,y,h} +$
$\sum_r \sum_y \sum_h[-Mv^{33}_{r,y,h} -$
$\left(M - Q_{r,y,h}K_{r,y,h}^{(MAX)}\right)v^{34}_{r,y,h}]\theta^{23}_{r,y,h} +$
$\sum_r \sum_y \sum_{h=1}[-Mv^{35}_{r,y,h} - (M - RA_r -$
$IG_r)v^{36}_{r,y,h}]\theta^{24}_{r,y,h} + \sum_r \sum_y \sum_{h>1}[-Mv^{37}_{r,y,h} -$
$(M - RA_r)v^{38}_{r,y,h}]\theta^{25}_{r,y,h} +$
$\sum_r \sum_y \sum_{h=1}[-Mv^{39}_{r,y,h} - (M - RA_r +$
$IG_r)v^{40}_{r,y,h}]\theta^{26}_{r,y,h} + \sum_r \sum_y \sum_{h>1}[-Mv^{41}_{r,y,h} -$
$(M - RA_r)v^{42}_{r,y,h}]\theta^{27}_{r,y,h} + \sum_l \sum_y \sum_h[-Mw^{8}_{l,y,h} -$
$\left(M - K_l^{(MAX)}\right)w^{9}_{l,y,h}]\theta^{28}_{l,y,h} +$
$\sum_l \sum_y \sum_h[-Mw^{10}_{l,y,h} -$
$\left(M - K_l^{(MAX)}\right)w^{11}_{l,y,h}]\theta^{29}_{l,y,h} +$
$\sum_l \sum_y \sum_h[-Mw^{12}_{l,y,h} - Mw^{13}_{l,y,h}]\theta^{30}_{l,y,h} +$
$\sum_y \sum_h[-Mw^{14}_{y,h} - \sum_s \sum_f (M{+}CH_s^{(MIN)} -$
$K_f^{(MAX)} + PS_y)w^{15}_{y,h}]\theta^{31}_{y,h} + \sum_y \sum_h[-Mw^{16}_{y,h} -$
$\sum_s \sum_d (M{+}DCH_s^{(MIN)} - D_{d,y,h}^{(MAX)} + NS_y)w^{17}_{y,h}]\theta^{32}_{y,h}$

(36c)

$\sum_s \sum_y \sum_h RC_s^{(UP)}u^{1}_{s,y,h} +$
$\sum_s \sum_y \sum_h RC_s^{(DN)}u^{2}_{s,y,h} - \sum_s \sum_y (FC_s^{(CAP)} +$
$RC_s^{(UP)} + RC_s^{(DN)})u^{11}_{s,y} - \sum_s \sum_y FC_s^{(EN)}u^{12}_{s,y} -$
$\sum_s \sum_y E^{(ST)}u^{5}_{s,y,h=1} + \sum_s \sum_y \sum_h DCH_s^{(MIN)}u^{9}_{s,y,h} +$
$\sum_s \sum_y \sum_h CH_s^{(MIN)}u^{10}_{s,y,h} - \sum_s \sum_y K_s^{(MAX)}u^{13}_{s,y} -$
$\sum_s \sum_y E_s^{(MAX)}u^{15}_{s,y} - \sum_f [\sum_y \sum_h (VC_f - RC_f^{(UP)} -$
$RC_f^{(DN)})Tv^{1}_{f,y,h}]/(1+i)^{y-1} -$
$\sum_f \sum_y \sum_h K_f^{(MAX)}v^{2}_{f,y,h} - \sum_f \sum_y \sum_{h=1}\left(RA_f +\right.$
$\left.IG_f\right)v^{3}_{f,y,h} - \sum_f \sum_y \sum_{h>1} RA_f v^{4}_{f,y,h} -$
$\sum_f \sum_y \sum_{h=1}\left(RA_f - IG_f\right)v^{5}_{f,y,h} -$
$\sum_f \sum_y \sum_{h>1} RA_f v^{6}_{f,y,h} +$
$\sum_d [\sum_y \sum_h P^{(MAX)}Tv^{7}_{d,y,h}]/(1+i)^{y-1} -$
$\sum_d \sum_y \sum_h D_{d,y,h}^{(MAX)}v^{8}_{d,y,h} - \sum_r [\sum_y \sum_h V_r T v^{9}_{r,y,h}]/$
$(1+i)^{y-1} - \sum_r \sum_y \sum_h Q_{r,y,h}K_{r,y,h}^{(MAX)}v^{10}_{r,y,h} -$
$\sum_r \sum_y \sum_{h=1}(RA_r + IG_r)v^{11}_{r,y,h} -$
$\sum_r \sum_y \sum_{h>1} RA_r v^{12}_{r,y,h} - \sum_r \sum_y \sum_{h=1}(RA_r -$
$IG_r)v^{13}_{r,y,h} - \sum_r \sum_y \sum_{h>1} RA_r v^{14}_{r,y,h} -$
$\sum_l \sum_y \sum_h K_l^{(MAX)}\left(w^{1}_{l,y,h} + w^{2}_{l,y,h}\right) +$
$\sum_s \sum_f \sum_y \sum_h \left(CH_s^{(MIN)} - K_f^{(MAX)} + PS_y\right)w^{6}_{y,h} +$
$\sum_s \sum_d \sum_y \sum_h \left(DCH_s^{(MIN)} - D_{d,y,h}^{(MAX)} + NS_y\right)w^{7}_{y,h} +$
$\sum_s \sum_y \sum_h[-Mu^{16}_{s,y,h} -$
$\left(M + RC_s^{(UP)}\right)u^{17}_{s,y,h}]\theta^{1}_{s,y,h} +$
$\sum_s \sum_y \sum_h[-Mu^{18}_{s,y,h} -$
$\left(M + RC_s^{(DN)}\right)u^{19}_{s,y,h}]\theta^{2}_{s,y,h} +$
$\sum_s \sum_y \sum_{h=1}[-Mu^{20}_{s,y,h} - Mu^{21}_{s,y,h}]\theta^{3}_{s,y,h} +$
$\sum_s \sum_y \sum_{h>1}[-Mu^{22}_{s,y,h} - Mu^{23}_{s,y,h}]\theta^{4}_{s,y,h} +$
$\sum_s \sum_y \sum_h[-Mu^{24}_{s,y,h} - Mu^{25}_{s,y,h}]\theta^{5}_{s,y,h} +$
$\sum_s \sum_y \sum_h[-Mu^{26}_{s,y,h} - Mu^{27}_{s,y,h}]\theta^{6}_{s,y,h} +$
$\sum_s \sum_y \sum_h[-Mu^{28}_{s,y,h} -$
$\left(M + DCH_s^{(MIN)}\right)u^{29}_{s,y,h}]\theta^{7}_{s,y,h} +$
$\sum_s \sum_y \sum_h[-Mu^{30}_{s,y,h} -$
$\left(M + CH_s^{(MIN)}\right)u^{31}_{s,y,h}]\theta^{8}_{s,y,h} + \sum_s \sum_y[-Mu^{32}_{s,y} -$
$\left(M - FC_s^{(CAP)} - RC_s^{(UP)} - RC_s^{(DN)}\right)u^{33}_{s,y}]\theta^{9}_{s,y} +$
$\sum_s \sum_y[-Mu^{34}_{s,y} - \left(M - FC_s^{(EN)}\right)u^{35}_{s,y}]\theta^{10}_{s,y} +$
$\sum_s \sum_y[-Mu^{36}_{s,y} - \left(M - K_s^{(MAX)}\right)u^{37}_{s,y}]\theta^{11}_{s,y} +$
$\sum_s \sum_y[-Mu^{38}_{s,y} - Mu^{39}_{s,y}]\theta^{12}_{s,y} + \sum_s \sum_y[-Mu^{40}_{s,y} -$
$\left(M - E_s^{(MAX)}\right)u^{41}_{s,y}]\theta^{13}_{s,y} + \sum_f \sum_y \sum_h[-Mv^{15}_{f,y,h} -$
$\frac{\left(M-(VC_f-RC_f^{(UP)}-RC_f^{(DN)})T\right)}{(1+i)^{y-1}} v^{16}_{f,y,h}]\theta^{14}_{f,y,h} +$
$\sum_f \sum_y \sum_h[-Mv^{17}_{f,y,h} -$
$\left(M - K_f^{(MAX)}\right)v^{18}_{f,y,h}]\theta^{15}_{f,y,h} +$
$\sum_f \sum_y \sum_{h=1}[-Mv^{19}_{f,y,h} - \left(M - RA_f -\right.$
$\left.IG_f\right)v^{20}_{f,y,h}]\theta^{16}_{f,y,h} + \sum_f \sum_y \sum_{h>1}[-Mv^{21}_{f,y,h} -$
$\left(M - RA_f\right)v^{22}_{f,y,h}]\theta^{17}_{f,y,h} +$
$\sum_f \sum_y \sum_{h=1}[-Mv^{23}_{f,y,h} - \left(M - RA_f +\right.$
$\left.IG_f\right)v^{24}_{f,y,h}]\theta^{18}_{f,y,h} + \sum_f \sum_y \sum_{h>1}[-Mv^{25}_{f,y,h} -$
$\left(M - RA_f\right)v^{26}_{f,y,h}]\theta^{19}_{f,y,h} + \sum_d \sum_y \sum_h[-Mv^{27}_{d,y,h} -$
$\frac{(M+P^{(MAX)}T)}{(1+i)^{y-1}} v^{28}_{d,y,h}]\theta^{20}_{d,y,h} + \sum_d \sum_y \sum_h[-Mv^{29}_{d,y,h} -$
$\left(M - D_{d,y,h}^{(MAX)}\right)v^{30}_{d,y,h}]\theta^{21}_{d,y,h} +$
$\sum_r \sum_y \sum_h[-Mv^{31}_{r,y,h} - \frac{(M-V_rT)}{(1+i)^{y-1}} v^{32}_{r,y,h}]\theta^{22}_{r,y,h} +$
$\sum_r \sum_y \sum_h[-Mv^{33}_{r,y,h} -$
$\left(M - Q_{r,y,h}K_{r,y,h}^{(MAX)}\right)v^{34}_{r,y,h}]\theta^{23}_{r,y,h} +$
$\sum_r \sum_y \sum_{h=1}[-Mv^{35}_{r,y,h} - (M - RA_r -$
$IG_r)v^{36}_{r,y,h}]\theta^{24}_{r,y,h} + \sum_r \sum_y \sum_{h>1}[-Mv^{37}_{r,y,h} -$
$(M - RA_r)v^{38}_{r,y,h}]\theta^{25}_{r,y,h} +$

$$\sum_r \sum_y \sum_{h=1}[-Mv^{39}_{r,y,h} - (M - RA_r + IG_r)v^{40}_{r,y,h}]\theta^{26}_{r,y,h} + \sum_r \sum_y \sum_{h>1}[-Mv^{41}_{r,y,h} - (M - RA_r)v^{42}_{r,y,h}]\theta^{27}_{r,y,h} + \sum_l \sum_y \sum_h[-Mw^{8}_{l,y,h} - (M - K_l^{(MAX)})w^{9}_{l,y,h}]\theta^{28}_{l,y,h} + \sum_l \sum_y \sum_h[-Mw^{10}_{l,y,h} - (M - K_l^{(MAX)})w^{11}_{l,y,h}]\theta^{29}_{l,y,h} + \sum_l \sum_y \sum_h[-Mw^{12}_{l,y,h} - Mw^{13}_{l,y,h}]\theta^{30}_{l,y,h} + \sum_y \sum_h[-Mw^{14}_{y,h} - \sum_s \sum_f (M + CH_s^{(MIN)} - K_f^{(MAX)} + PS_y)w^{15}_{y,h}]\theta^{31}_{y,h} + \sum_y \sum_h[-Mw^{16}_{y,h} - \sum_s \sum_d (M + DCH_s^{(MIN)} - D^{(MAX)}_{d,y,h} + NS_y)w^{17}_{y,h}]\theta^{32}_{y,h} \le 0$$

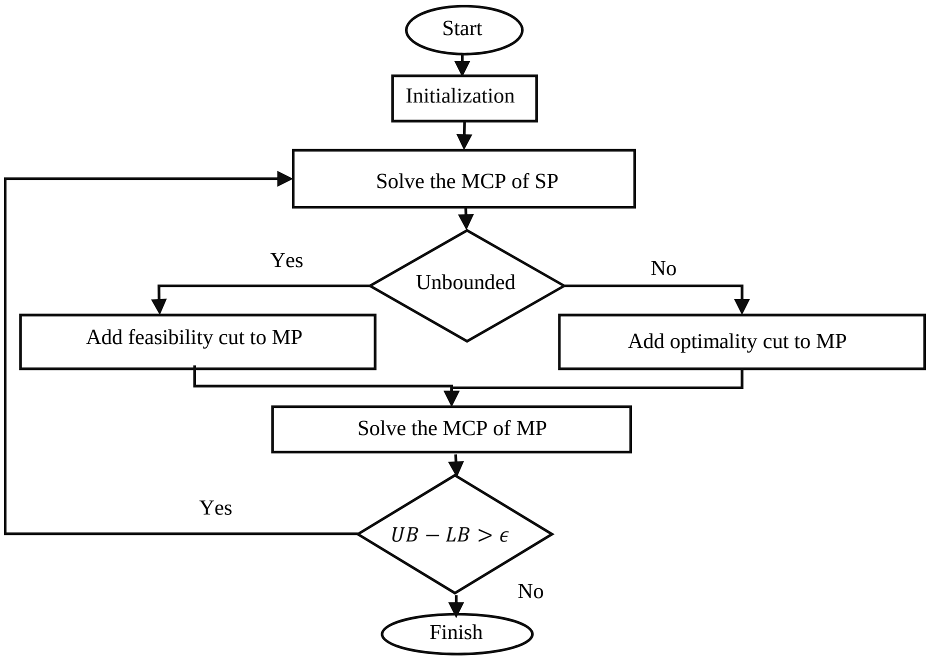

Fig. 1. The Benders decomposition algorithm

5. Results and discussion

This section focuses on evaluating the performance of the proposed model for several case studies. Section 5.1 presents illustrative examples of the 3-node and 300-node systems, and Section 5.2 presents the computational results for IEEE case studies. The case study data is obtained from MATPOWER. These case studies run on a computer with an Intel Core i7 processor and 256 GB of RAM. GAMS software is used to code all case studies. The LP model is solved using the Cplex solver, and the MCP model is solved using the Path solver. Furthermore, the 3-node example system and the actual case study are solved using the Benders decomposition technique.

5.1. *Illustrative example*

Fig. 2 shows a single-line diagram of the 3-node example system. As seen in Fig. 2, the example system has two conventional generators, two RE generators, one PHS, and one demand unit. Node 3 is designated as a slack node in this system.

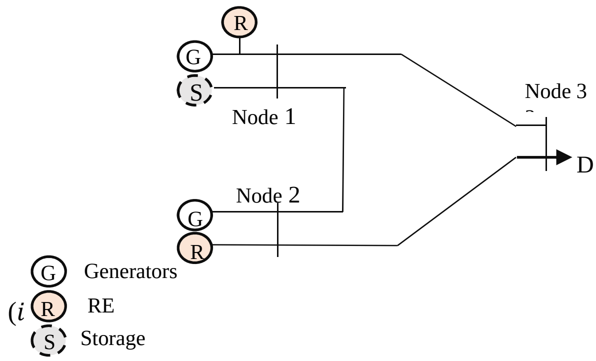

Fig. 2. The single-line diagram of 3-node system

The proposed model is solved for one year ($Y, T = 1$) with two time periods ($h = 2$). The value of $P^{(MAX)}$, $D^{(MAX)}_{d,y,h}$ in both time periods, and PS_y and NS_y are considered 2000 ($ per MWh), 5000 (MW), 1000 (MW), and 1000 (MW), respectively. In addition, the interest rate) is 0.08. The other input data for this system are presented in Table 1-Table 3.

Table 1.
The input data of conventional generators in the 3-node example system

f	VC_f	IG_f	RA_f	$RC_f^{(UP)}$	$RC_f^{(DN)}$	$K_f^{(MAX)}$
1	30	50	1000	15	15	4000
2	20	50	1000	0	0	4000

Table 2.
The input data of RE generators in the 3-node example system

r	h	V_r	IG_r	RA_r	$Q_{r,y,h}$	$K_{r,y,h}^{(MAX)}$
1	1	30	0.5	1000	1	5000
	2				0	5000
2	1	20	0.5	1000	0.5	5000
	2				1	5000

Table 3.
The input data of the PHS system in the 3-node example system

s	$FC_s^{(CAP)}$	$FC_s^{(EN)}$	$RC_s^{(UP)}$	$RC_s^{(DN)}$	$E_s^{(MAX)}$	$CH_s^{(MIN)}$	$DCH_s^{(MIN)}$	$K_s^{(MAX)}$	SL_s	$E^{(ST)}$
1	100	200	100	100	4000	0	0	4000	0.7	50

Table 4-Table 8 show the results of solving the 3-node example system. The load in the first period is 4135.5 MW, and the load in the second period is 4100 MW, which according to the input data in the second period, the PHS contributes 35 MW to its supply.

Table 4.
Results of conventional generators in the 3-node example system

f	h	$gen_{f,y,h}$	$\alpha_{f,y,h}$	$\phi_{f,y,h}^{(1)}$	$\phi_{f,y,h}^{(2)}$
1	1	1050	0	6000	0
	2	2050	0	4000	0
2	1	1050	0	2000	0
	2	2049.5	0	0	0

As can be seen from the calculated value of the objective function (social welfare) of 16.06 M$, the demand is met by conventional generators, RE generators, and PHS. Table 4 shows that conventional generators are active in both periods. In the first and second periods, 1050 and 2050 MW of the 4000 MW capacities of the conventional generators are used, respectively.

Because of the limited access to RE generators, RE generator 1 is inactive in the second period, as shown in Table 5.

Table 5.
Results of RE generators in the 3-node example system

r	h	$gen_{r,y,h}$	$\beta_{f,y,h}$	$\phi_{r,y,h}^{(1)}$	$\phi_{r,y,h}^{(2)}$
1	1	1000	0	0	0
	2	0	5996	0	1998
2	1	1000.5	0	1990	0
	2	0.5	0	0	5

The capacity of the PHS system is determined to be 35 MW in Table 6 based on the model's input data and constraints.

Table 6.
Results of the PHS system in the 3-node example system

s	h	$\xi_{s,y,h}$	$ch_{s,y,h}$	$dch_{s,y,h}$	$e_{s,y,h}^{(st)}$	$\mu_{s,y,h}$	$\iota_{s,y,h}$	$\delta_{s,y,h}$	$\varpi_{s,y,h}$	$k_{s,y}^{(in)}$
1	1	1260	0	35	0	0	300	1318	0	35
	2	2714.286	0	0	0	0	0	0	0	

Table 7.
Results of transmission lines in the 3-node example system

	$l=1,h=1$	$l=1,h=2$	$l=2,h=1$	$l=2,h=2$	$l=3,h=1$	$l=3,h=2$
$\chi_{l,y,h}$	0	660.606	0	0	0	0
$flow_{l,y,h}$	11.385	0	2041.38	2029.5	2052.765	2029.5
$o_{l,y,h}$	0	0	0	0	0	0
$\pi_{l,y,h}$	0	0	0	0	0	0

The load in the first period is 4135.5 MW, and the load in the second period is 4100 MW. According to the input data in the second period, the PHS contributes 35 MW in supplying electrical energy (see Table 8).

Table 8.
Others results in the 3-node example system

d	h	$ld_{d,y,h}$	$\tau_{d,y,h}$	$\lambda_{y,h}$	$\eta_{y,h}$	$\zeta_{y,h}$
1	1	4135.5	0	2000	0	0
	2	4100	0	2000	0	0

The results of solving the 3-node example system using the CPLEX solver and the Benders decomposition are the same. However, for problems with large dimensions, the CPLEX solver cannot solve and achieve the desired result; in this case, the Benders decomposition is recommended. The following section looks at a 300-node example system with MATPOWER input data.

Table 9.
Results of Benders decomposition for the 300-node example system

s	y	h	$e_{s,y}^{(in)}$	$k_{s,y}^{(in)}$	$ch_{s,y,h}$	$dch_{s,y,h}$	$e_{s,y,h}^{(st)}$
1	1,2,3,…,10	1	106.96	156.2	81.372	0	106.96
		2			0	74.798	0
2	1,2,3,…,10	1	78.641	95.91	40.916	0	78.641
		2			0	54.994	0
3	1,2,3,…,10	1	32.355	81.19	0	34.965	0
		2			46.221	0	32.355
4	1,2,3,…,10	1	50	50	0	0	50
		2			0	0	0
5	1,2,3,…,10	1	113.084	169.2	90.12	0	113.09
		2			0	79.08	0

There are 69 conventional generators, two RE generators, five PHSs, and 202 demand units in the 300-node example system. This system considers two time periods ($h = 2$) and a 10-year planning horizon ($Y = 10$). The CPLEX solver is unable to solve in an acceptable time. Therefore, the Benders decomposition is used.

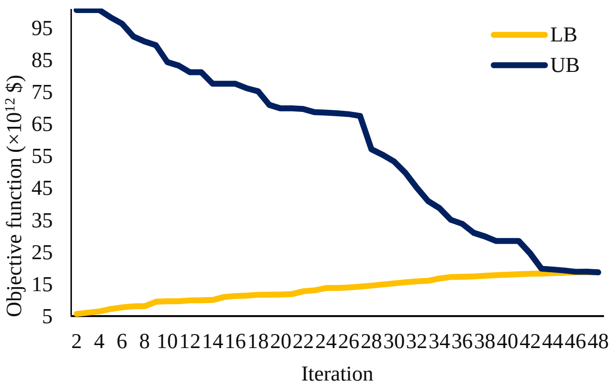

Fig. 3. Convergence graph

Table 9 displays the Benders decomposition results obtained in GAMS. Fig. 3 also depicts the convergence graph of Benders decomposition. This graph shows how time steps evolve during the problem-solving process.

5.2. Computational results for the IEEE case studies

This section compares the performance of MILP and MCP models. The performance is evaluated with various numbers of nodes obtained from MATPOWER. MATPOWER provided all the input data. In IEEE 3-node, IEEE 4-node, IEEE 6-node, IEEE 14-node, and IEEE 30-node example systems, the performance of the MILP and MCP models are compared. These two models are evaluated based on two criteria, the computational time and the value of the objective function (social welfare) obtained from solving the model. Finally, the optimal PHSS investment results from the MCP model for IEEE case studies are presented.

These findings illustrate that our MCP model and the original MILP model are equivalent, confirming the binary relaxation approach proposed in our paper. Table 10 shows the computational time required to solve the MILP and MCP models in the case studies, and Fig. 4 compares their SW values in various case studies. As expected, the computation time grows with the size of the problem, as shown in Table 10.

Table 10.
Computational time (CT) for the MILP and MCP models in seconds

	3-node	4-node	6-node	14-node	30-node
CT for MILP model	0.174	0.179	0.180	0.343	1.273
CT for MCP model	0.016	0.166	0.175	0.348	3.317

As shown in Fig. 4, increasing the dimensions of the problem improves the performance of the MCP model over the MILP model.

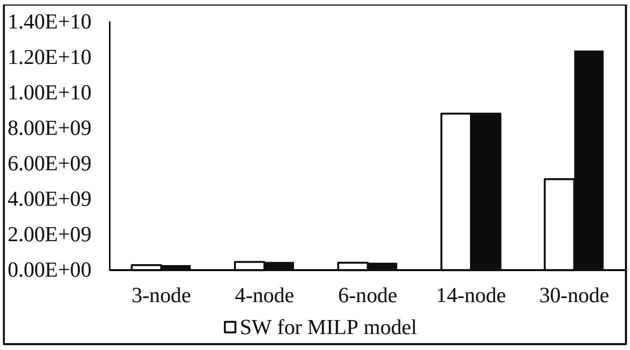

Fig. 4. Comparison of the SW values of the MILP and MCP models in various case studies

Section 5.1 discusses the results of the IEEE 3-node system (*Illustrative example*). Table 11-Table 14 presents the outcomes of solving the MCP model for storage in other case studies. These findings show PHS activity in all case studies, emphasizing the importance of considering PHS systems when meeting electricity demand.

Table 11 .
The outcomes of solving the MCP model for the IEEE 4-node system PHS

s	y	h	$e_{s,y}^{(in)}$	$k_{s,y}^{(in)}$	$ch_{s,y,h}$	$dch_{s,y,h}$	$e_{s,y,h}^{(st)}$
		1	2446.55	1997.53	0	35	0
1	1	2	2446.55	1997.53	1497.53	0	1048.27
		3	2446.55	1997.53	1997.53	0	2446.55

The PHS in Table 11's IEEE 4-node system acts as a generator in the first period and a pump in the later periods. As shown in Table 12, the PHS is active in the IEEE 6-node system during the second period of each year.

Table 12.
The outcomes of solving the MCP model for the IEEE 6-node system PHS

s	y	h	$e_{s,y}^{(in)}$	$k_{s,y}^{(in)}$	$ch_{s,y,h}$	$dch_{s,y,h}$	$e_{s,y,h}^{(st)}$
		1	0	35	0	35	0
	1	2	0	35	0	0	0
		3	0	35	0	0	0
1		1	0	35	0	35	0
	2	2	0	35	0	0	0
		3	0	35	0	0	0

A 3-year lifetime and two storages are considered in the IEEE 14-node system. According to Table 13, both of them are investments with a capacity of 35 MW.

Table 13.
The outcomes of solving the MCP model for the IEEE 14-node system PHS

s	y	h	$e_{s,y}^{(in)}$	$k_{s,y}^{(in)}$	$ch_{s,y,h}$	$dch_{s,y,h}$	$e_{s,y,h}^{(st)}$
		1	0	36.925	0	37.282	0
		2	0	36.925	0	0.037	0.004
	1	3	0	36.925	0.006	0	0
		4	0	36.925	0	0	0
1		5	0	36.925	0	0	0
		6	0	36.925	0	0	0
		1	0	36.942	0	36.811	0
	2	2	0	36.942	0	0.093	0.004
		3	0	36.942	0.006	0	0
		4	0	36.942	0	0	0

		5	0	36.942	0	0	0
		6	0	36.942	0	0	0
	3	1	0	36.969	0	36.698	0
		2	0	36.969	0	0.135	0.004
		3	0	36.969	0.006	0	0
		4	0	36.969	0	0	0
		5	0	36.969	0	0	0
		6	0	36.969	0	0	0
2	1	1	2.995	35.362	0	29.266	4.898
		2	2.995	35.362	0	1.353	0.984
		3	2.995	35.362	0	0.111	0.089
		4	2.995	35.362	0.004	0	0.308
		5	2.995	35.362	0	0	0.208
		6	2.995	35.362	0	0	0.249
	2	1	3.197	35.366	0	28.881	4.983
		2	3.197	35.366	0	1.428	0.998
		3	3.197	35.366	0	0.111	0.082
		4	3.197	35.366	0	0	0.009
		5	3.197	35.366	0.005	0	0.317
		6	3.197	35.366	0	0	0.273
	3	1	3.187	35.269	0	28.808	4.975
		2	3.187	35.269	0	1.483	1.007
		3	3.187	35.269	0	0.111	0.089
		4	3.187	35.269	0.004	0	0.307
		5	3.187	35.269	0	0	0.167
		6	3.187	35.269	0	0	0.174

Table 14 shows that allocating PHS systems in the IEEE 30-node system results in higher social welfare in the network. The capacity of all three PHS systems is expanded in this system, and they remain operational throughout the study's duration.

Table 14.
The outcoms of solving the MCP model for the IEEE 30-node system PHS

s	y	h	$e_{s,y}^{(in)}$	$k_{s,y}^{(in)}$	$ch_{s,y,h}$	$dch_{s,y,h}$	$e_{s,y,h}^{(st)}$
1	1,2,3	1	25	110.804	0	60.331	25
		2	25	110.804	0	60.331	0
		3	25	110.804	50.473	0	0
		4	25	110.804	50.473	0	0
		5	25	110.804	0	0	0
		6	25	110.804	0	0	0
		7	25	110.804	0	0	0
		8	25	110.804	0	0	0
		9	25	110.804	0	0	0
		10	25	110.804	0	0	0
2	1,2,3	1	25	25	0	25	25
		2	25	25	0	25	0
		3	25	25	0	0	0
		4	25	25	0	0	0
		5	25	25	0	0	0
		6	25	25	0	0	0
		7	25	25	0	0	0
		8	25	25	0	0	0
		9	25	25	0	0	0
		10	25	25	0	0	0
3	1,2,3	1	25	139.32	0	72.073	25
		2	25	139.32	0	72.073	0
		3	25	139.32	67.247	0	0
		4	25	139.32	67.247	0	0
		5	25	139.32	0	0	0
		6	25	139.32	0	0	0
		7	25	139.32	0	0	0
		8	25	139.32	0	0	0
		9	25	139.32	0	0	0
		10	25	139.32	0	0	0

6. Conclusion

This paper proposes two models for determining the optimal storage system investment. The report begins with a MILP model of the storage investment problem and then offers a relaxation technique to convert it to an equivalent LP model. Because of the LP model's convexity, the equivalent LP model is much easier to solve than the original MILP model. For large case studies, the LP investment model is more promising. Then, an equivalent MCP model suitable for decentralized market-based studies is developed. Because the MCP model is computationally challenging to solve, the Benders decomposition algorithm is proposed to address the computational challenges.

A 3-node system example is solved to evaluate the performance of the proposed models. The Benders decomposition technique solves the model for a 300-node system that the CPLEX cannot solve. 3, 4, 6, 14, and 30-node case studies are solved to compare the performance of the MILP and MCP models. These case studies are also solved using the Benders decomposition technique.

The results show that the proposed models perform optimally in the case studies examined. The activity of storage devices in all case studies suggests that storage devices should be considered to meet the increase in electricity demand in the intermittent renewable future.

This work can be expanded by improving the Benders decomposition technique and considering other storage technologies in our proposed models.

References

Abadie, L.M., & Goicoechea, N. (2022). Optimal management of a mega pumped hydro storage system under stochastic hourly electricity prices in the Iberian Peninsula. Energy, 252, 123974, doi: 10.1016/J.ENERGY.2022.123974.

Ali, S., Stewart, R.A., & Sahin, O. (2021). Drivers and barriers to the deployment of pumped hydro energy storage applications: Systematic literature review. Clean. Eng. Technol., 5, 100281, doi: 10.1016/J.CLET.2021.100281.

Arteaga, J., Zareipour, H., & Amjady, N. (2021). Energy Storage as a Service: Optimal sizing for Transmission Congestion Relief. Appl. Energy, 298, doi: 10.1016/j.apenergy.2021.117095.

Barbour, E., Wilson, I.A.G., Radcliffe, J., Ding, Y., & Li, Y. (2016). A review of pumped hydro energy storage development in significant international electricity markets. Renew. Sustain. Energy Rev., 61, 421–432, doi: 10.1016/J.RSER.2016.04.019.

Benalcazar, P. (2021). Optimal sizing of thermal energy storage systems for CHP plants considering specific investment costs: A case study. Energy, 234, doi: 10.1016/j.energy.2021.12132.

Canales, F.A., Jurasz, J.K., Guezgouz, M., & Beluco, A. (2021). Cost-reliability analysis of hybrid pumped-battery storage for solar and wind energy integration in an island community. Sustain. Energy Technol. Assessments, doi: 10.1016/j.seta.2021.101062.

Dvorkin, Y., Fernandez-Blanco, R., Wang, Y., Xu, B., S. Kirschen, D., Pandzic, H., Watson, J.P., & Silva-Monroy, C.A. (2018). Co-planning of investments in transmission and merchant energy storage. IEEE Trans. Power Syst., doi: 10.1109/TPWRS.2017.2705187.

Ferris, M.C., & Munson, T.S. (2000). Complementarity problems in GAMS and the PATH solver. J. Econ. Dyn. Control, doi: 10.1016/s0165-1889(98)00092-x.

Fertig, E., Heggedal, A.M., Doorman, G., & Apt, J. (2014). Optimal investment timing and capacity choice for pumped hydropower storage. Energy Syst., doi: 10.1007/s12667-013-0109-x.

Gardiner, D., Schmidt, O., Heptonstall, P., Gross, R., & Staffell, I. (2019). Quantifying the impact of policy on the investment case for residential electricity storage in the UK. Journal of Energy Storage, 27, doi: 10.1016/j.est.2019.101140.

Gaudard, L. (2015). Pumped-storage project: A short to long term investment analysis including climate change. Renewable and Sustainable Energy Reviews., doi: 10.1016/j.rser.2015.04.052.

Gravelle, H.S.E. (1976). The Peak Load Problem with Feasible Storage. Econ. J., 86 (342), 256, doi: 10.2307/2230746.

Guittet, M., Capezzali, M., Gaudard, L., Romerio, F., Vuille, F., & Avellan, F. (2016). Study of the drivers and asset management of pumped-storage power plants historical and geographical perspective. Energy, 111, 560–579, doi: 10.1016/J.ENERGY.2016.04.052.

Haas, J., Prieto-Miranda, L., Ghorbani, N., & Breyer, C.(2022). Revisiting the potential of pumped-hydro energy storage: A method to detect economically attractive sites. Renew. Energy, 181, 182–193, doi: 10.1016/J.RENENE.2021.09.009.

Hassan, A., & Dvorkin, Y. (2018). Energy Storage Siting and Sizing in Coordinated Distribution and Transmission Systems. IEEE Trans. Sustain. Energy, 9 (4), 1692–1701, doi: 10.1109/TSTE.2018.2809580.

Hesamzadeh, M.R., Rosellon, J., & Vogelsang, I. (2020). An introduction to transmission network investment in the new market regime. in Lecture Notes in Energy, doi: 10.1007/978-3-030-47929-9_1.

Huang, Q., Xu, Y., & Courcoubetis, C. (2020). Stackelberg competition between merchant and regulated storage investment in wholesale electricity markets. Appl. Energy, doi: 10.1016/j.apenergy.2020.114669.

Hunt, J.D., Zakeri, B., Nascimento, A., & Brandão, R. (2022). Pumped hydro storage (PHS). Storing Energy with Spec. Ref. to Renew. Energy Sources, 37–65, doi: 10.1016/B978-0-12-824510-1.00008-8.

Javed, M.S., Zhong, D., Ma, T., Song, A., & Ahmed, S. (2020). Hybrid pumped hydro and battery storage for renewable energy based power supply system. Appl. Energy, 257, 114026, doi: 10.1016/J.APENERGY.2019.114026.

Kalvelagen, E. (2002). Benders decomposition with GAMS. Amsterdam Optim. Model. Gr. Washington, DC, USA

Korpås, M., & Botterud, A. (2020). Optimality Conditions and Cost Recovery in Electricity Markets with Variable Renewable Energy and Energy Storage. MIT Cent. Energy Environ. Policy Res., no. Mar 2020, [Online]. Available: http://ceepr.mit.edu/files/papers/2020-005.pdf

Lin, S. Ma, T., & hahzad Javed, M.S. (2020). Prefeasibility study of a distributed photovoltaic system with pumped hydro storage for residential buildings. Energy Convers. Manag., 222, 113199,doi: 10.1016/J.ENCONMAN.2020.113199.

Liu Y., & Woo, C.K. (2017). California's renewable generation and pumped hydro storage's profitability. Electr. J., 30 (3), 15–22, doi: 10.1016/J.TEJ.2017.02.009.

Liu, X., Li, N., Mu, H., Li, M., & Liu, X. (2021). Techno-energy-economic assessment of a high capacity offshore wind-pumped-storage hybrid power system for regional power system. J. Energy Storage, 41, 102892, doi: 10.1016/J.EST.2021.102892.

Liu, J., Chen, X., Xiang, Y., Huo, D., & Liu, J. (2021). Optimal planning and investment benefit analysis of shared energy storage for electricity retailers. Int. J. Electr. Power Energy Syst., doi: 10.1016/j.ijepes.2020.106561.

Mousavi, N., Kothapalli, G., Habibi, M. Khiadani, D., & Das, C.K. (2019). An improved mathematical model for a pumped hydro storage system considering electrical, mechanical, and hydraulic losses. Appl. Energy, doi: 10.1016/j.apenergy.2019.03.015.

Murphy, J. (2013). Benders, Nested Benders & Stochastic Programming: An Intuitive Introduction. arXiv Prepr. arXiv1312.3158, 2013, [Online]. Available: http://arxiv.org/abs/1312.3158

Nazari, A.A., Keypour, R., & Amjady, N. (2021). Joint investment of community energy storage systems in distribution networks using modified Nash bargaining theory. Appl. Energy, 301, doi: 10.1016/j.apenergy.2021.117475.

Nguyen, D.T. (1976). Problems of Peak Loads and Inventories.. Bell J Econ, 7 (1), 242–248, doi: 10.2307/3003199.

Rehman, S., Al-Hadhrami, L.M., & Alam, M.M. (2015). Pumped hydro energy storage system: A technological review. Renewable and Sustainable Energy Reviews, doi: 10.1016/j.rser.2014.12.040.

Saber, H., Moeini-Aghtaie, M., & Ehsan, M. (2018). Developing a multi-objective framework for expansion planning studies of distributed energy storage systems (DESSs). Energy, 157, 1079–1089, doi: 10.1016/j.energy.2018.06.081.

Spisto, A. & Hrelja, N. (2016). The Economic and Environmental Assessment of Electricity Storage Investments. Any Need for Policy Incentives?.

Energy Procedia, 106, 122–133, doi: 10.1016/J.EGYPRO.2016.12.110.

Steffen B., & Weber, C. (2013). Efficient storage capacity in power systems with thermal and renewable generation. Energy Econ., 36, 556–567, doi: 10.1016/j.eneco.2012.11.007.

Tómasson, E., Hesamzadeh, M.R., & Wolak, F.A. (2020). Optimal offer-bid strategy of an energy storage portfolio: A linear quasi-relaxation approach. Appl. Energy, 260, 114251, doi: 10.1016/J.APENERGY.2019.114251.

Xu, B., Wang, Y., Dvorkin, Y., Fernandez-Blanco, R., Silva-Monroy, C.A., Watson, J.P., & S. Kirschen. (2017). Scalable Planning for Energy Storage in Energy and Reserve Markets. IEEE Trans. Power Syst., 32 (6), 4515–4527, doi: 10.1109/TPWRS.2017.2682790.

Yang, Z., Sun, G., Behrens, P., Qstergaard, P.A., Egusquiza, M., Egusquiza, E., Xu, B., Chen, D., & Patelli, W. (2021). The potential for photovoltaic-powered pumped-hydro systems to reduce emissions, costs, and energy insecurity in rural China. Energy Convers. Manag. X, 11, 100108, doi: 10.1016/J.ECMX.2021.100108.

Zhang X., & Conejo, A.J. (2018). Coordinated investment in transmission and storage systems representing long- and short-term uncertainty. IEEE Trans. Power Syst., 33 (6), 7143–7151, doi: 10.1109/TPWRS.2018.2842045.

This article can be cited: Goudarzi, Z., Bagherinejad, J., Rafiee, M., & Souratgar, A. A. (2023). Optimizing Investment of Pumped Hydro Storage System for Renewable Energy Future. *Journal of Optimization in Industrial Engineering, 16*(1), 167-184. doi: 10.22094/joie.2023.1974939.2022